

Efficient Inference Using Large Language Models with Limited Human Data: Fine-Tuning then Rectification

Lei Wang

Foster School of Business, University of Washington, Seattle, WA, lei0603@uw.edu

Zikun Ye

Foster School of Business, University of Washington, Seattle, WA, zikunye@uw.edu

Jinglong Zhao

Questrom School of Business, Boston University, Boston, MA, jinglong@bu.edu

Driven by recent advances in artificial intelligence (AI), a growing literature has demonstrated the potential for using large language models (LLMs) as scalable surrogates to generate human-like responses in many business applications. Two common approaches to improve the performance of LLMs include: *fine-tuning*, which aligns LLMs more closely with human responses, and *rectification*, which corrects biases in LLM outputs. In this paper, we develop a two-stage framework that combines fine-tuning and rectification, and optimally allocates limited labeled samples across the two stages. Unlike the conventional objective that minimizes the mean squared prediction errors, we propose to minimize the variance of the prediction errors as the fine-tuning objective, which is optimal for the downstream rectification stage. Building on this insight, we leverage the scaling law of fine-tuning to optimally allocate the limited labeled human data between the fine-tuning and rectification stages. Our empirical analysis validates the fine-tuning scaling law and confirms that our proposed optimal allocation rule reliably identifies the optimal sample allocation. We demonstrate substantial efficiency gains in estimation and inference performance relative to fine-tuning or rectification alone, or to employing the standard mean-squared error objective within the fine-tuning then rectification framework, resulting in significant cost savings for reliable business decisions.

Key words: Large Language Models, Fine-Tuning, Prediction-Powered Inference

History: This version: December 30, 2025

1. Introduction

Businesses routinely conduct surveys to inform managerial decisions, such as conjoint analysis (Green and Srinivasan 1990), new product development (Wind and Mahajan 1997), and pricing (Wertenbroch and Skiera 2002). Traditional survey methods are often recognized to be costly, time-consuming, and difficult to scale.

The rapid advancement of artificial intelligence (AI), particularly in Large Language Models (LLMs), has offered a potential solution to this bottleneck: the use of LLMs as human surrogates. Rather than solely relying on recruiting thousands of human participants, businesses can use LLMs to simulate human-like responses, such as evaluating products and expressing preferences, with

minimal latency and near-zero marginal cost. This solution has proven successful well beyond survey studies. It enables a wide range of business applications, including estimating demand curves and price elasticities (Gui and Toubia 2023), modeling discrete choices for assortment optimization (Wang et al. 2024), and content optimization (Ye et al. 2025).

There is growing empirical evidence supporting the use of LLMs as human surrogates. Trained on vast corpora of human-generated text, LLMs have demonstrated the capacity to encode complex human behavioral patterns and social norms. Recent studies confirm that these models can closely approximate human responses in diverse market research and social science applications (Brand et al. 2023, Li et al. 2024, Toubia et al. 2025, Peng et al. 2025). As a result, LLM-as-surrogate has become an increasingly attractive tool for accelerating insight generation across different domains, allowing managers to conduct “virtual” market tests and experiments with unprecedented speed and scale. There are a growing number of commercial platforms, such as Synthetic Users, Delve AI, and Quantilope, which offer tools that leverage human-like AI participants to automate market research.

To serve as effective surrogates, LLMs must be properly aligned with the target human population. However, off-the-shelf LLMs are often not suited for this task, as their pretraining optimizes for next-token prediction rather than human behavioral alignment; furthermore, their reliance on public corpora means they lack access to proprietary datasets, often leading to knowledge gaps in specialized domains. Consequently, empirical studies document consistent and systematic discrepancies between LLM-generated outputs and survey responses (Motoki et al. 2024, Li et al. 2025). Furthermore, LLM predictions are also highly sensitive to prompt designs, where minor syntactic changes can yield widely divergent outcomes (Brucks and Toubia 2023). The accuracy of LLM responses could be improved through inference-time prompting techniques that do not update model parameters, such as chain-of-thought prompting to elicit step-by-step reasoning (Wei et al. 2022), in-context learning with several demonstrations to clarify the task (Brown et al. 2020), and persona prompting to simulate specific subpopulations (Peng et al. 2025). However, their ability to consistently and accurately reflect human respondents remains questionable in the literature (Pezeshkpour and Hruschka 2024, Ye et al. 2025, Krsteski et al. 2025). These limitations of inference-time prompting techniques highlight the need for methodological advances that leverage LLMs as human surrogates more effectively. Broadly speaking, existing approaches can be characterized into two methods: *fine-tuning*, and *rectification*.

Fine-tuning aligns an LLM by explicitly updating its underlying parameters during a post-training phase using labeled samples. This method has proven successful in bridging the gap between model outputs and human responses across various business applications (Ye et al. 2025, Cheng et al. 2025). Its adoption has been further accelerated by parameter-efficient fine-tuning

(PEFT) methods, such as LoRA (Hu et al. 2022), which trains only small low-rank adapters and thus is computationally more efficient. Recent studies confirm that PEFT achieves performance comparable to full fine-tuning at a fraction of the computational cost (Han et al. 2024). However, fine-tuning relies heavily on the availability of high-quality, task-specific labeled samples. Empirical evidence indicates that fine-tuning performance generally follows a power-law scaling relationship (Kaplan et al. 2020, Hernandez et al. 2021, Hoffmann et al. 2022, Zhang et al. 2024). This implies diminishing marginal returns: the value of each additional labeled sample decreases as the total size of labeled samples grows. Moreover, fine-tuning alone does not provide statistical guarantees on the magnitude of errors that still remain in the model, making it difficult to quantify the reliability of the aligned model. From a business perspective, the absence of guarantees makes it difficult to assess whether errors are small enough to support an important decision.

In contrast to fine-tuning, the rectification method does not update the underlying parameters of the pretrained LLM. Instead, the rectification method treats the LLM as a black box, uses labeled samples to quantify the errors of the LLM, and rectifies the outputs from the LLM using the quantified errors post hoc. One of the most prominent examples of the rectification method is prediction-powered inference (PPI), which combines LLM predictions with labeled samples to construct unbiased estimators and valid confidence intervals (Angelopoulos et al. 2023a). This focus on bias correction and inference reliability is particularly valuable for business decisions, where even small systematic errors can be costly. Similar to fine-tuning, one primary requirement for PPI is also the availability of high-quality labeled samples. Because the variance of the PPI estimator scales inversely with the sample size, this approach also exhibits diminishing marginal returns: the value of each additional labeled sample decreases as the total size of labeled samples grows.

Since both fine-tuning and rectification are subject to diminishing marginal returns, relying exclusively on either method could be inefficient. This motivates us to combine both fine-tuning and rectification methods to take advantage of the rapid initial gains of each method, efficiently allocating our limited labeled data among two methods.

1.1. A Fine-Tuning then Rectification Framework

In this paper, we propose a new *fine-tuning then rectification* framework designed to combine both methods. At a high level, our framework partitions the labeled samples into two disjoint subsets: the first is used to fine-tune the LLM, and the second is used in the subsequent rectification stage.

We analyze how the variance of the final rectification estimator depends on the quality of the fine-tuned LLM’s surrogate. This analysis allows us to identify the use of residual variance as the fine-tuning objective, which is optimal for the downstream rectification stage. Conceptually similar to the predict-then-optimize framework (Elmachtoub and Grigas 2022, Ferreira et al. 2016),

we demonstrate that the standard mean-squared error training objective is not aligned with the downstream task of rectification.

Building on this insight, we propose a data-driven procedure that leverages empirical scaling laws to determine the optimal sample allocation between fine-tuning and rectification. The literature has extensively studied the scaling law, showing that LLM performance improves in smooth, predictable ways as model size and sample size increase, often following simple power-law patterns in both pretraining and fine-tuning stages (Kaplan et al. 2020, Hernandez et al. 2021, Hoffmann et al. 2022, Zhang et al. 2024). In our setting, the scaling law describes how the quality of the fine-tuned LLM improves with additional labeled data, which enables us to identify the optimal allocation of limited labeled samples between fine-tuning and rectification that minimizes the variance of the final estimator. Furthermore, we characterize the properties of the optimal allocation rule and analyze the magnitude of variance reduction under our proposed framework.

To the best of our knowledge, this is the first work to formally analyze the theoretical interplay between fine-tuning and rectification. While recent independent work by Krsteski et al. (2025) empirically observes that combining these methods yields improvements, their approach relies on standard fine-tuning procedures that do not take into account the downstream rectification task. In contrast, our framework derives a fine-tuning objective explicitly tailored to the rectification stage and provides a rigorous method for optimally allocating labeled samples between the two stages.

We validate our framework through an empirical study using the Wine Reviews dataset to estimate the average ratings in the population. This task mirrors a day-to-day challenge faced by product teams. When retailers select which stock-keeping units (SKUs) to sell in their stores, they usually need to understand the perceived product quality at scale without incurring large monetary costs and delays associated with extensive human labeling.

Our empirical analysis shows four main findings. First, we empirically confirm a strong and stable scaling law in LLM fine-tuning with our proposed variance-based training objective, making the marginal value of additional labeled data highly predictable for budget planning. Second, we validate our optimal sample allocation rule. We show that the theoretical optimum derived from the scaling law accurately guides the empirical optimal allocation. Third, our proposed framework consistently outperforms all relevant benchmarks, including the sample mean estimator using only the small labeled dataset, standard fine-tuning, vanilla PPI, and the alternative fine-tuning then rectification method but under the standard mean-squared error objective. These performance gains translate into substantial sample savings: our method reduces the labeling budget by 45% to 66% compared to the sample mean estimator, to achieve the same level of accuracy. Finally, we show that the choice of fine-tuning objective is important in our fine-tuning then rectification

framework. Replacing the MSE fine-tuning objective with our proposed variance-based objective brings 18% to 54% variance reduction across different data budget settings.

Roadmap

The rest of the paper is structured as follows. In Section 2, we review the literature. In Section 3, we formalize the problem setup and define the combined fine-tuning and rectification estimator. In Section 4, we derive the main theoretical results of our framework. We analyze the estimator’s variance to motivate a variance-based fine-tuning objective. We then leverage empirical scaling laws to derive the optimal sample allocation rule, and establish the theoretical conditions under which our method outperforms standard baselines. In Section 5, we extend this framework from mean estimation to the more general M -estimation problems. In Section 6, we conduct empirical analysis on the Wine Reviews dataset. In Section 7, we conclude the paper.

2. Related Literature

In this section, we review three lines of literature that are most related to our work.

LLM Fine-Tuning. Fine-tuning has become a standard approach to adapt pretrained language models to downstream tasks by updating model parameters using labeled samples (Brown et al. 2020, Ouyang et al. 2022). For large models, parameter-efficient fine-tuning methods, such as LoRA (Hu et al. 2022) introduce task-specific low-rank matrix adapters while freezing most parameters, making fine-tuning computationally efficient in practice. A large empirical literature on neural scaling laws shows that model performance tends to follow smooth power-law relationships with model size, data size, and compute scale (Kaplan et al. 2020, Hernandez et al. 2021, Hoffmann et al. 2022, Zhang et al. 2024), providing us with a parametric function to use the size of labeled samples to predict the model quality.

Other fine-tuning methods, such as RLHF and DPO, update models using a separate trained reward model or preference data (Ouyang et al. 2022, Rafailov et al. 2023). Beyond vanilla fine-tuning with commonly used objective functions such as mean-squared errors and cross-entropy losses, recent works have started to modify objectives to target downstream tasks directly. For example, Vafa et al. (2025) propose a debiased fine-tuning method for using foundation models to estimate the gender wage gap. In our proposed framework, we focus on the setting where an LLM is used as a surrogate within a PPI estimator and design a fine-tuning objective that directly minimizes the variance governing the efficiency of the final PPI estimator.

Prediction-Powered Inference. The PPI method combines a small set of labeled samples with a large set of model predictions to construct unbiased estimators and confidence intervals, while treating the prediction model as a potentially biased black box (Angelopoulos et al. 2023a). Follow-up works, such as the PPI++ method from Angelopoulos et al. (2023b), develop more efficient

variants. Recent research further connects PPI to the classical surrogate-outcome literature, showing that PPI-type estimators can be interpreted as using predictions as surrogates and proposing re-calibration procedures that achieve improved efficiency (Ji et al. 2025). Our work builds on this line of research by taking the prediction model to be an LLM that can itself be improved via fine-tuning, and by explicitly designing both the fine-tuning objective and the allocation of labeled data to minimize the asymptotic variance of the PPI estimator.

PPI is only one rectification method. There are other post-hoc rectification methods. For example, Wang et al. (2024) propose a transfer-learning-based method to correct the bias from LLMs. In this paper, we focus on the standard PPI framework for clarity, though our core insights extend to other post-hoc rectification approaches.

LLMs for Business Applications. There is a fast growing literature that evaluates whether LLMs can serve as surrogates for human respondents in high-fidelity business applications, ranging from demand estimation to consumer choice modeling. Brand et al. (2023) examine the use of LLMs to estimate willingness to pay. They document mixed results: LLMs can reproduce aggregate patterns reasonably well, but they generate insufficient heterogeneity across individuals even after fine-tuning. And the fine-tuned models struggle to extrapolate beyond the training distribution. Other work studies whether LLMs can reproduce human preferences or attitudes in specific domains, such as brand perception (Li et al. 2024), computational social science, (Argyle et al. 2023, Ziems et al. 2024), and content experiments (Ye et al. 2025), all highlighting their potential to augment, rather than replace, human data. At the same time, several recent papers also document important limitations. Gui and Toubia (2023) raise endogeneity concerns when using LLMs to simulate human behavior from a causal-inference perspective. Wang et al. (2024) show that while LLM-generated responses are useful for data augmentation in choice modeling, they often exhibit systematic biases relative to human samples and require careful calibration.

Our contribution is methodological and complements this literature. Rather than assessing LLMs as stand-alone survey respondents, we study how to combine fine-tuning and post-hoc rectification when LLM outputs are used as surrogate responses. We further show how to optimally allocate scarce human-labeled data between improving the surrogate model and correcting its residual biases to obtain accurate estimates and make reliable decisions.

3. Problem Setup

We consider a mean estimation problem in a setting where we have access to both a small, labeled dataset and a large, unlabeled dataset. We extend this mean estimation problem to the more general M -estimation problem in Section 5. Let there be n samples in the small labeled dataset $\mathcal{N} = \{(\mathbf{X}_i, Y_i)\}_{i=1}^n$, where each sample (\mathbf{X}_i, Y_i) is an independent and identically distributed (i.i.d.)

replica of a representative random variable (\mathbf{X}, Y) sampled from a joint distribution $(\mathbf{X}, Y) \sim \mathcal{F}$. Let there be m samples in the large unlabeled dataset $\mathcal{M} = \{\tilde{\mathbf{X}}_j\}_{j=1}^m$, where each sample $\tilde{\mathbf{X}}_j$ is an i.i.d. replica of a representative random variable \mathbf{X} sampled from the marginal distribution $\mathbf{X} \sim \mathcal{F}_{\mathbf{X}}$, where $\mathcal{F}_{\mathbf{X}}$ stands for the marginal distribution over \mathbf{X} according to the joint distribution \mathcal{F} . Let $\mathcal{X} \times \mathcal{Y}$ be the set that \mathcal{F} takes values from. We also have access to an LLM predictor $f: \mathcal{X} \rightarrow \mathcal{Y}$ that is trained on data independent of both datasets. This LLM predictor f can take unstructured data, such as textual information, as inputs. See our empirical application in Section 6 for an illustration of the inputs and outputs of an LLM predictor.

Given these two datasets and the predictor, there are two families of methods for leveraging LLMs as human surrogates: fine-tuning, which adapts the model using the small labeled dataset, and post-hoc rectification, which corrects model predictions without modifying the model itself.

1. **Fine-Tuning (FT).** We can use the small labeled dataset to fine-tune the LLM predictor, and then use the fine-tuned LLM predictor to construct estimators.
2. **Prediction-Powered Inference (PPI).** We can use the small labeled dataset to measure the errors of the LLM predictor, and then rectify the errors on the large unlabeled dataset.

In this paper, we proposed to combine fine-tuning and prediction-powered inference to achieve the merits of both approaches. As each sample in the small labeled dataset can only be used either in fine-tuning (FT) or in prediction-powered inference (PPI), we study the optimal sample allocation of the n samples between FT and PPI.

For any $0 < s < n$, let s be the number of samples we allocate to FT. Consequently, $n - s$ is the number of samples we allocate to PPI. Let $f^{(s)}: \mathcal{X} \rightarrow \mathcal{Y}$ be the LLM predictor that is fine-tuned on s samples of the small labeled dataset. We propose to use the prediction-powered estimator (Angelopoulos et al. 2023a) based on the fine-tuned predictor $f^{(s)}(\cdot)$, defined as follows,

$$\hat{\mu} = \frac{1}{n-s} \sum_{i=1}^{n-s} (Y_i - f^{(s)}(\mathbf{X}_i)) + \frac{1}{m} \sum_{j=1}^m f^{(s)}(\tilde{\mathbf{X}}_j). \quad (1)$$

It is easy to see that $\hat{\mu}$ as defined in (1) is unbiased,

$$\mathbb{E}[\hat{\mu}] = \mathbb{E}[Y] - \mathbb{E}[f^{(s)}(\mathbf{X})] + \mathbb{E}[f^{(s)}(\mathbf{X})] = \mathbb{E}[Y],$$

where the first equality is because \mathbf{X}_i from the small labeled dataset and $\tilde{\mathbf{X}}_j$ from the large unlabeled dataset are sampled from the same distribution. As the estimator $\hat{\mu}$ is unbiased, the mean-squared error of the estimator is equal to its variance. A lower variance directly implies more accurate estimates, narrower confidence intervals, and more efficient use of scarce labeled data. In the following, our goal is to combine fine-tuning and PPI to make the most efficient use of limited human labels.

4. Our Method

In this section, we begin by analyzing the variance of the PPI estimator and derive its implications for how the LLM should be fine-tuned in Section 4.1. We then use the scaling law in fine-tuning to characterize the optimal allocation of labeled samples between fine-tuning and PPI in Section 4.2, assuming the exact fine-tuning scaling law is known. We provide a data-driven method to estimate the parameters of the scaling law in Online Appendix EC.2. Finally, we analyze the performance of our proposed method in Section 4.3 and provide inference results in Section 4.4.

4.1. A New Loss Function for Fine-Tuning

We start by examining the variance of $\hat{\mu}$ as defined in (1), following the same analysis in Angelopoulos et al. (2023a).

$$\begin{aligned}
& \mathbb{E}[(\hat{\mu} - \mathbb{E}[Y])^2] \\
&= \mathbb{E}\left[\left(\frac{1}{n-s} \sum_{i=1}^{n-s} (Y_i - f^{(s)}(\mathbf{X}_i)) + \frac{1}{m} \sum_{j=1}^m f^{(s)}(\tilde{\mathbf{X}}_j) - \mathbb{E}[Y]\right)^2\right] \\
&= \mathbb{E}\left[\left(\frac{1}{n-s} \sum_{i=1}^{n-s} (Y_i - f^{(s)}(\mathbf{X}_i) + \mathbb{E}[f^{(s)}(\mathbf{X})] - \mathbb{E}[Y]) + \frac{1}{m} \sum_{j=1}^m (f^{(s)}(\tilde{\mathbf{X}}_j) - \mathbb{E}[f^{(s)}(\mathbf{X})])\right)^2\right] \\
&= \frac{1}{n-s} \sum_{i=1}^{n-s} \mathbb{E}\left[\left(Y_i - f^{(s)}(\mathbf{X}_i) + \mathbb{E}[f^{(s)}(\mathbf{X})] - \mathbb{E}[Y]\right)^2\right] + \frac{1}{m} \sum_{j=1}^m \mathbb{E}\left[\left(f^{(s)}(\tilde{\mathbf{X}}_j) - \mathbb{E}[f^{(s)}(\mathbf{X})]\right)^2\right] \\
&= \frac{1}{n-s} \text{Var}\left(Y - f^{(s)}(\mathbf{X})\right) + \frac{1}{m} \text{Var}\left(f^{(s)}(\mathbf{X})\right) \tag{2}
\end{aligned}$$

where the third equality is because $(Y_i - f^{(s)}(\mathbf{X}_i))$ and $f^{(s)}(\tilde{\mathbf{X}}_j)$ are independent.

Because we have a large unlabeled dataset, the second term is small when m is large. So we focus our attention primarily on the first term, $\frac{1}{n-s} \text{Var}(Y - f^{(s)}(\mathbf{X}))$. Recall that each sample in the small labeled dataset can only be used either in FT or in PPI. We make the following two observations regarding the benefits of allocating more samples to the FT stage and to the PPI stage, which present a trade-off in sample allocation.

1. The term $\frac{1}{n-s} \text{Var}(Y - f^{(s)}(\mathbf{X}))$ decreases when $n - s$ increases. This observation indicates that the more data we use toward PPI, the smaller this term becomes.
2. The term $\frac{1}{n-s} \text{Var}(Y - f^{(s)}(\mathbf{X}))$ decreases when $\text{Var}(Y - f^{(s)}(\mathbf{X}))$ decreases. This observation indicates that the more data we use toward FT, the higher quality is the fine-tuned predictor $f^{(s)}(\cdot)$, which then makes $\text{Var}(Y - f^{(s)}(\mathbf{X}))$ smaller.

It is worth noting that the bias of the fine-tuned predictor $f^{(s)}(\cdot)$ does not play an important role in the expression in (2). Even when the fine-tuned predictor $f^{(s)}(\cdot)$ is biased, our estimator $\hat{\mu}$ as defined in (1) can still have a small variance, as long as the variance of $Y - f^{(s)}(\mathbf{X})$ is small. See Example 1 below.

EXAMPLE 1 (FINE-TUNING A BIASED PREDICTOR). We consider an extreme case where the fine-tuned predictor always under-predicts by a constant, that is, there exists $c > 0$ such that $Y - f^{(s)}(\mathbf{X}) = c$. In this case, the mean-squared error $E[(Y - f^{(s)}(\mathbf{X}))^2] = c^2$ can be large. But the variance $\text{Var}(Y - f^{(s)}(\mathbf{X})) = 0$ is always equal to zero. This implies that a predictor with high bias can still be optimal for the prediction-powered estimator, provided that the bias is a *constant* with zero variance. \square

Example 1 motivates the use of variance $\text{Var}(Y - f^{(s)}(\mathbf{X}))$, rather than the traditional mean-squared error (MSE), as the loss function for fine-tuning. We refer to this variance $\text{Var}(Y - f^{(s)}(\mathbf{X}))$ as the “residual variance.”

REMARK 1. The two objectives are closely related. In particular, when the model class allows for additive constant shifts (e.g., through an intercept or a last-layer bias), minimizing MSE implicitly also minimizes the residual variance. In an ideal setting with large enough data and a flexible intercept, the two objectives essentially lead to the same solution. However, the two objectives can behave differently in more practical settings where data is not large enough, or when the model is trained under regularization or early stopping. The residual variance objective is invariant to additive shifts of the predictions, which aligns naturally with the PPI framework that can explicitly correct any systematic bias using labeled data. Training using the MSE prioritizes fitting the mean level of the responses, whereas training using the residual variance prioritizes reducing the residual dispersion. Since the leading residual variance term of the PPI estimator depends on the dispersion of the residuals rather than their mean, this distinction can be significant. In Section 6.4, we empirically compare the two objectives and demonstrate the benefits of using the residual variance as the objective. We also note that for general M -estimation problems the target objective is no longer a simple mean, so the appropriate training objective differs from the standard MSE objective.

4.2. Optimal Sample Allocation

Fine-tuning is a flexible method that allows us to use variance $\text{Var}(Y - f^{(s)}(\mathbf{X}))$ as the loss function. Empirically, it is widely accepted that fine-tuning can effectively reduce the loss of the LLM predictor following a smooth power-law relationship, i.e., scaling law (Kaplan et al. 2020, Hernandez et al. 2021, Hoffmann et al. 2022, Zhang et al. 2024),

$$\text{Var}(Y - f^{(s)}(\mathbf{X})) = as^{-\alpha} + b,$$

where $\alpha, a > 0$, $b \geq 0$ are task-specific constants. Note that scaling law formulations typically incorporate model size as an independent variable. In our setting, we treat the size of the underlying foundation model as fixed, because size choices are typically constrained by practical considerations

such as inference cost and available base models. Moreover, many open-weight foundation models offer only a small set of discrete size options. OpenAI’s gpt-oss provides only 20B-parameter and 120B-parameter variants (OpenAI 2025). Thus, we abstract away from the model size decision and treat it as given.

When the constants are known, we can minimize variance in the expression in (2) by solving the following univariate optimization problem,

$$\min_{s \in (0, n)} \frac{\text{Var}(Y - f^{(s)}(\mathbf{X}))}{n - s} = \min_{s \in (0, n)} \frac{as^{-\alpha} + b}{n - s}. \quad (3)$$

We can express the optimal solution to (3) through the following theorem.

THEOREM 1 (Optimal Allocation Rule). *The optimal solution to (3), s^* , is given as the unique solution to*

$$\alpha a n s^{-\alpha-1} - (\alpha + 1) a s^{-\alpha} - b = 0. \quad (4)$$

The optimal solution s^* can easily be calculated through numerically solving equation (4) via a binary search, using the property that the left-hand side of equation (4) is monotone decreasing in s . The proof can be found in Online Appendix EC.1.

Next, we investigate the properties of the optimal allocation $s^*(a, b, \alpha, n)$ and its dependence on scaling law parameters a, b, α and the total sample size n .

PROPOSITION 1 (Characterization of the Optimal Allocation Rule). *The unique solution $s^*(a, b, \alpha, n)$ to the optimization problem (3) has the following properties:*

- (i) $s^*(a, b, \alpha, n)$ is nondecreasing in a , and strictly increasing in a whenever $b > 0$.
- (ii) $s^*(a, b, \alpha, n)$ is strictly decreasing in b .
- (iii) $s^*(a, b, \alpha, n)$ is strictly increasing in n .
- (iv) In the special case when $b = 0$,

$$\frac{s^*}{n} = \frac{\alpha}{\alpha + 1},$$

which is independent of a and n .

- (v) The fine-tuning fraction s^*/n is nondecreasing in a (strictly increasing if $b > 0$), strictly decreasing in b , and nonincreasing in n . Specifically, if $b > 0$, the fraction vanishes asymptotically

$$\lim_{n \rightarrow \infty} \frac{s^*}{n} = 0.$$

Moreover, its derivative with respect to n is uniformly bounded if $\alpha < 1$:

$$0 \geq \frac{\partial}{\partial n} \left(\frac{s^*}{n} \right) \geq -\frac{\alpha}{\alpha + 1} \frac{b}{a} n^{\alpha-1}. \quad (5)$$

The proof of Proposition 1 can be found in Online Appendix EC.1. The first three properties describe how the optimal number of fine-tuning samples, s^* , reacts to changes in the parameters a , b , and n . First, s^* is nondecreasing in a . Since a represents the scaling law's steepness, a higher value implies the model gains more performance per unit of data. Accordingly, it is optimal to allocate more samples to fine-tuning. Second, s^* is strictly decreasing in b . The parameter b can be interpreted as the noise floor, which is due to the intrinsic variance of the data or approximation error of the model. If b increases, it is optimal to allocate fewer samples for fine-tuning. Third, it is intuitive that when the total available samples n grow, the samples allocated to fine-tuning naturally grow with it.

The last two properties characterize the behavior of the fine-tuning fraction, s^*/n . Property (iv) establishes a theoretical baseline: in the case where there is no irreducible variance, i.e., $b = 0$, the optimal fraction is a perfect constant, $\alpha/(\alpha + 1)$, which depends solely on the power-law exponent. This value serves as the upper bound for the allocation ratio. In the more common case where $b > 0$, property (v) reveals that the ratio s^*/n deviates from this baseline. It is strictly decreasing in both b and n . Theoretically, this fraction vanishes asymptotically as the dataset grows indefinitely, i.e., $\lim_{n \rightarrow \infty} s^*/n = 0$. This implies that given an infinite budget of labeled data, the optimal fine-tuning set size s^* would grow indefinitely, yet the fraction s^*/n will asymptotically vanish.

For practical purposes, Equation (5) provides an important bound on this behavior. It establishes that the rate of this decay is uniformly bounded by a term proportional to b/a . This implies that if b/a is small, the optimal ratio remains close to the theoretical ceiling $\alpha/(\alpha + 1)$ if the dataset size n is not too large.

4.3. Performance Analysis of FT+PPI

Theorem 1 shows that, under the scaling law, the variance minimization problem has a unique interior minimizer $s^* \in (0, n)$. While a closed-form solution for s^* is not available, Proposition 1 characterizes the properties of the optimal fine-tuning sample size and ratio.

We now turn to the performance analysis of the proposed method. We study conditions under which the FT+PPI estimator outperforms the naive sample mean in terms of variance, given that both methods are unbiased. In the following analysis, the scaling law parameters a, b, α are known quantities. In practice, these parameters can be estimated from a data-driven “ramp-up” procedures. See Online Appendix EC.2.

For a given fine-tuning budget s , we define the variance-based goodness-of-fit as

$$R^2(s) = 1 - \frac{\text{Var}(Y - f^{(s)}(\mathbf{X}))}{\text{Var}(Y)}.$$

Given n labeled samples (\mathbf{X}_i, Y_i) and m unlabeled samples $\tilde{\mathbf{X}}_j$, the FT+PPI estimator $\hat{\mu}$ utilizes the fine-tuned model $f^{(s)}$. Assuming the number of unlabeled samples m is sufficiently large, the

variance of the estimator is dominated by the prediction error on the small labeled dataset (see expression (2)). On the other hand, the baseline sample mean estimator, $\hat{\mu}_{\text{mean}} = \frac{1}{n} \sum_{i=1}^n Y_i$, has variance $\text{Var}(\hat{\mu}_{\text{mean}}) = \text{Var}(Y)/n$.

Proposition 2 below provides a necessary and sufficient condition on $R^2(s)$ for the FT+PPI estimator to outperform the sample mean estimator. It shows that the goodness-of-fit $R^2(s)$ obtained in the fine-tuning stage is important for deciding whether the subsequent PPI stage reduces variance relative to the baseline. The proof of Proposition 2 is given in Online Appendix EC.1.

PROPOSITION 2 (Criterion for Variance Reduction). *Fix n and $s \in (0, n)$, and assume the number of unlabeled samples is large $m \rightarrow \infty$. Then,*

$$\text{Var}(\hat{\mu}) < \text{Var}(\hat{\mu}_{\text{mean}}) \iff R^2(s) > \frac{s}{n}.$$

Proposition 2 shows that FT+PPI strictly outperforms the sample mean estimator if and only if the $R^2(s)$ from the fine-tuned model exceeds the fraction of labeled data consumed by fine-tuning, s/n . Intuitively, Proposition 2 suggests that the variance reduction achieved by the fine-tuned model $f^{(s)}(\mathbf{X})$ must outweigh the statistical cost of reducing the sample size from n to $n - s$.

Proposition 2 assumes an asymptotic regime where the number of unlabeled samples $m \rightarrow \infty$, implying that the second variance term in equation (2) vanishes. This assumption is justified by the fact that the costs of acquiring unlabeled data and computing LLM responses are typically negligible compared to the costs of collecting human labels. We can also easily incorporate the variance contribution from finite m into Proposition 2.

Proposition 2 provides a condition for variance reduction. Yet it does not directly suggest whether this condition is achievable.

Next, we incorporate the scaling law to derive the boundary conditions for improvement. For notational convenience, denote $\sigma^2 = \text{Var}(Y)$. The proof of Proposition 3 is given in Online Appendix EC.1.

PROPOSITION 3 (Conditions for Variance Reduction under Scaling Laws). *Suppose the residual variance follows the scaling law $\text{Var}(Y - f^{(s)}(\mathbf{X})) = as^{-\alpha} + b$ with parameters $a, \alpha > 0$, $b \geq 0$, and assume the number of unlabeled samples $m \rightarrow \infty$. Define the variance discriminant function $q(s)$ as follows*

$$q(s) := \underbrace{\sigma^2(n - s)}_{\text{Baseline Contribution}} - \underbrace{n(as^{-\alpha} + b)}_{\text{FT+PPI Contribution}}, \quad s \in (0, n).$$

Then the following properties hold:

- (i) *Equivalence: There exists a valid allocation $s \in (0, n)$ (and thus an optimal s^*) such that FT+PPI strictly improves upon the sample mean estimator if and only if $\max_{s \in (0, n)} q(s) > 0$.*

(ii) *Feasibility Condition:* Due to the strict concavity of $q(s)$, the maximum is unique. There exists a valid allocation $s \in (0, n)$ (and thus an optimal s^*) such that FT+PPI strictly improves upon the sample mean estimator if and only if:

$$\frac{b}{\sigma^2} < 1 - \left(1 + \frac{1}{\alpha}\right) \left(\frac{a\alpha n^{-\alpha}}{\sigma^2}\right)^{1/(\alpha+1)}. \quad (6)$$

Condition (6) serves as a verifiable decision rule, showing that the variance reduction of FT+PPI depends on the following two factors. First, the task learnability, represented by the ratio of irreducible error b/σ^2 , plays a limiting role. The parameter b dictates the best achievable error the fine-tuned model given enough data. If the irreducible error b is too high relative to the inherent data variance σ^2 , the model's predictive power will never suffice to justify the “cost” of removing samples from the PPI estimation set to fine-tuning. Second, the total dataset size n determines the threshold for success. In Condition (6), the sample size n appears in the negative term on the right-hand side. As n increases, the term proportional to $n^{-\alpha/(\alpha+1)}$ decreases, causing the entire right-hand side to increase and approach 1. Consequently, a larger n raises the feasibility threshold, making it easier for the condition to hold. This implies that even for tasks with moderate to hard learnability, FT+PPI can become viable if the dataset becomes sufficiently large. We illustrate the above two factors through Example 2 below.

EXAMPLE 2 (APPLYING PROPOSITION 3 TO EVALUATE FT+PPI). To demonstrate how Proposition 3 can be used as a diagnostic tool to determine the viability of FT+PPI, consider an example with a variance $\sigma^2 = 1$, a learning rate constant $a = 1$, and a scaling exponent $\alpha = 1$. Under these conditions, the feasibility condition simplifies to $b < 1 - 2/\sqrt{n}$. This formula translates to two observations:

1. *Effect of sample size n :* In a data-scarce regime where $n = 4$, the feasibility threshold becomes $1 - 2/2 = 0$. Since the noise floor $b \geq 0$, the condition $b < 0$ is impossible to satisfy. In this case, FT+PPI is strictly inferior to the classical sample mean regardless of the model's potential quality. However, as the sample size grows to $n = 100$, the threshold increases to 0.8, rendering the method feasible so long as the irreducible error $b < 0.8$.
2. *Effect of noise floor b :* Even with a larger sample size ($n = 100$), task difficulty remains a constraint. If the task is inherently noisy such that $b = 0.9$, the condition $0.9 < 0.8$ fails. This indicates that the irreducible error is too dominant to justify the cost of fine-tuning, even when more data is available.

This example shows that while the feasible region for FT+PPI expands as n increases, it remains fundamentally bounded by the inherent noise floor b of the prediction task. \square

Condition (6) also serves as a valuable diagnostic tool. In practice, one does not need to execute the entire two-stage fine-tuning and rectification procedures to determine whether it leads to variance reduction. Instead, by relying on prior knowledge of the task's scaling law or estimating the parameters a, b , and α on a subset of the data, we can evaluate whether Condition (6) holds. If the inequality is not satisfied, one should go with the standard sample mean estimator to avoid computational waste; if the inequality is satisfied, one can proceed with FT+PPI as variance reduction is theoretically achievable.

4.4. Inference

To conclude the discussion of our method, we state the inference method provided by Angelopoulos et al. (2023a) to construct a confidence interval for mean estimation.

First, we estimate the sample variance

$$\hat{\sigma}_{f^{(s)}}^2 = \frac{1}{m-1} \sum_{j=1}^m \left(f^{(s)}(\tilde{\mathbf{X}}_j) - \frac{1}{m} \sum_{j=1}^m f^{(s)}(\tilde{\mathbf{X}}_j) \right)^2$$

in the large unlabeled dataset. Second, we estimate the sample variance

$$\hat{\sigma}_{Y-f^{(s)}}^2 = \frac{1}{n-s-1} \sum_{i=1}^{n-s} \left(Y_i - f^{(s)}(\mathbf{X}_i) - \frac{1}{n-s} \sum_{i=1}^{n-s} (Y_i - f^{(s)}(\mathbf{X}_i)) \right)^2$$

in the small labeled dataset. Finally, for any $\delta \in (0, 1)$, we calculate the following confidence interval

$$\left[\hat{\mu} - z_{1-\frac{\delta}{2}} \sqrt{\frac{\hat{\sigma}_{Y-f^{(s)}}^2}{n-s} + \frac{\hat{\sigma}_{f^{(s)}}^2}{m}}, \hat{\mu} + z_{1-\frac{\delta}{2}} \sqrt{\frac{\hat{\sigma}_{Y-f^{(s)}}^2}{n-s} + \frac{\hat{\sigma}_{f^{(s)}}^2}{m}} \right].$$

Proposition 1 of Angelopoulos et al. (2023a) suggests that the confidence interval constructed in this way is asymptotically valid.

5. Extension to M -Estimation

In this section, we provide a more general framework for M -estimation. We follow the same problem setup as in Section 3. Instead of population mean estimation, we consider the estimation of a vector of d -dimensional parameters $\boldsymbol{\theta}^* \in \mathbb{R}^d$ defined as

$$\boldsymbol{\theta}^* = \arg \min_{\boldsymbol{\theta} \in \mathbb{R}^d} \mathbb{E}_{(\mathbf{X}, Y) \sim \mathcal{F}} [l(\mathbf{X}, Y; \boldsymbol{\theta})],$$

where $l(\mathbf{X}, Y; \boldsymbol{\theta})$ is the loss function that is twice differentiable with respect to $\boldsymbol{\theta}$ and such that the expected loss has a unique minimizer. The parameter vector $\boldsymbol{\theta}^* \in \mathbb{R}^d$ is thus the solution to the following first order condition

$$\mathbb{E}_{(\mathbf{X}, Y) \sim \mathcal{F}} [\boldsymbol{\psi}(\mathbf{X}, Y; \boldsymbol{\theta})] = \mathbf{0},$$

where $\boldsymbol{\psi}(\mathbf{X}, Y; \boldsymbol{\theta}) = \nabla_{\boldsymbol{\theta}} l(\mathbf{X}, Y; \boldsymbol{\theta})$ is the score function. We illustrate the above notations through the following examples.

EXAMPLE 3 (MEAN ESTIMATION). In the mean estimation problem, we would like to estimate the mean of an outcome $\theta = E[Y]$. Mean estimation is a special case of M -estimation where the loss function is defined as $l(\mathbf{X}, Y; \theta) = \frac{1}{2}(Y - \theta)^2$. In this case, the score function is given by $\psi(\mathbf{X}, Y; \theta) = \theta - Y$. The first order condition $E[\psi(\mathbf{X}, Y; \theta)] = 0$ implies that $\theta = E[Y]$, which is exactly the mean of an outcome. \square

EXAMPLE 4 (CATEGORICAL RESPONSE ESTIMATION). Estimating the distribution of categorical responses is fundamental in survey-based market research, such as determining the market share of d options (e.g., options A, B, C, D when $d = 4$) in a multiple-choice survey. Beyond surveys, such categorical response estimation problem is also useful in revenue management applications such as stock keeping unit (SKU) rationalization, where managers identify underperforming products based on their market shares (Lee et al. 1993, Lee and Tang 1997, Alfaro and Corbett 2003). Here, $Y \in [d]$ represents the selection of one specific option. We aim to estimate the probability vector $\boldsymbol{\theta} = (\Pr(Y = 1), \Pr(Y = 2), \dots, \Pr(Y = d))^\top$. This is a special case of M -estimation where the loss function is defined as $l(\mathbf{X}, Y; \boldsymbol{\theta}) = \sum_{l=1}^d \frac{1}{2}(\mathbb{1}\{Y = l\} - \theta_l)^2$. In this case, the score function is given by $\psi(\mathbf{X}, Y; \boldsymbol{\theta}) = \boldsymbol{\theta} - (\mathbb{1}\{Y = 1\}, \dots, \mathbb{1}\{Y = d\})^\top$. The first order condition $E[\psi(\mathbf{X}, Y; \boldsymbol{\theta})] = \mathbf{0}$ implies that $\boldsymbol{\theta} = (\Pr(Y = 1), \dots, \Pr(Y = d))^\top$, which recovers the categorical response probabilities. \square

EXAMPLE 5 (LINEAR REGRESSION). Linear regression is widely used in business applications. A classic use case is estimating the price-demand relationship (Gallego et al. 2019, Gui and Toubia 2023, Talluri and Van Ryzin 2006, Tirole 1988), where Y represents demand and \mathbf{X} represents product attributes (e.g., prices). Note that in our LLM framework, \mathbf{X} typically denotes the raw textual query given to LLMs. Here, with a slight abuse of notation, we let \mathbf{X} be the feature vectors extracted from the text, e.g., product profile and price. Linear regression is a special case of M -estimation where the loss function is defined as $l(\mathbf{X}, Y; \boldsymbol{\theta}) = \frac{1}{2}(Y - \mathbf{X}^\top \boldsymbol{\theta})^2$. In this case, the score function is given by $\psi(\mathbf{X}, Y; \boldsymbol{\theta}) = \mathbf{X}(\mathbf{X}^\top \boldsymbol{\theta} - Y)$. The first order condition $E[\psi(\mathbf{X}, Y; \boldsymbol{\theta})] = \mathbf{0}$ implies that $\boldsymbol{\theta} = E[\mathbf{X} \mathbf{X}^\top]^{-1} E[\mathbf{X} Y]$, which is the population ordinary least squares estimator. \square

EXAMPLE 6 (CHOICE MODEL ESTIMATION). Choice model estimation, particularly using the Multinomial Logit (MNL) model, is widely used in revenue management applications such as assortment optimization and pricing, where a manager chooses the SKUs and sets their prices to maximize profit, revenue, or market share (Berry et al. 1995, Gallego et al. 2019, Talluri and Van Ryzin 2006), as well as market research, e.g., recent work has also explored integrating LLMs with such choice models to analyze consumer choice behavior (Brand et al. 2023, Wang et al. 2024). In this problem, we observe samples drawn from the joint distribution of $(\mathbf{X}_1, \mathbf{X}_2, \dots, \mathbf{X}_K, Y)$, where $Y \in \{0, 1, \dots, K\}$ represents the choice among K options (with 0 denoting the no-purchase option). Similar to the linear regression example, while \mathbf{X} typically denotes the raw textual input in our framework, here we abuse notation to let $\mathbf{X}_k \in \mathbb{R}^d$ denote the feature vector for the k -th

option extracted from the text here. We aim to estimate the coefficients $\boldsymbol{\theta}$ in the standard MNL model:

$$\Pr(Y = k) = \frac{\exp(\mathbf{X}_k^\top \boldsymbol{\theta})}{1 + \sum_{\kappa=1}^K \exp(\mathbf{X}_\kappa^\top \boldsymbol{\theta})}, \quad \forall k \in [K].$$

MNL estimation is a special case of M -estimation where the loss function is defined as

$$l(\mathbf{X}_1, \mathbf{X}_2, \dots, \mathbf{X}_K, Y; \boldsymbol{\theta}) = \log \left(1 + \sum_{k=1}^K \exp(\mathbf{X}_k^\top \boldsymbol{\theta}) \right) - \sum_{k=1}^K \mathbf{X}_k^\top \boldsymbol{\theta} \mathbb{1}\{Y = k\}.$$

With some calculations, the score function is given by

$$\psi(\mathbf{X}_1, \mathbf{X}_2, \dots, \mathbf{X}_K, Y; \boldsymbol{\theta}) = \sum_{k=1}^K \left(\frac{\exp(\mathbf{X}_k^\top \boldsymbol{\theta})}{1 + \sum_{\kappa=1}^K \exp(\mathbf{X}_\kappa^\top \boldsymbol{\theta})} - \mathbb{1}\{Y = k\} \right) \mathbf{X}_k$$

The first order condition $\mathbb{E}[\psi(\mathbf{X}_1, \mathbf{X}_2, \dots, \mathbf{X}_K, Y; \boldsymbol{\theta})] = \mathbf{0}$ provides a moment condition to solve $\boldsymbol{\theta}$, which is usually implemented using numerical optimization algorithms such as the Newton-Raphson algorithm. \square

The prediction-powered M -estimator (Angelopoulos et al. 2023a) is defined as the solution to the rectified empirical risk minimization problem,

$$\hat{\boldsymbol{\theta}} = \arg \min_{\boldsymbol{\theta} \in \mathbb{R}^d} \left[\frac{1}{n-s} \sum_{i=1}^{n-s} \left(l(\mathbf{X}_i, Y_i; \boldsymbol{\theta}) - l(\mathbf{X}_i, f^{(s)}(\mathbf{X}_i); \boldsymbol{\theta}) \right) + \frac{1}{m} \sum_{j=1}^m l(\tilde{\mathbf{X}}_j, f^{(s)}(\tilde{\mathbf{X}}_j); \boldsymbol{\theta}) \right]. \quad (7)$$

It is easy to see that $\hat{\boldsymbol{\theta}}$ as defined in (7) is a consistent estimator. To see this, we focus on the right-hand side of (7) when both $(n-s) \rightarrow +\infty$ and $m \rightarrow +\infty$.

$$\begin{aligned} & \frac{1}{n-s} \sum_{i=1}^{n-s} \left(l(\mathbf{X}_i, Y_i; \boldsymbol{\theta}) - l(\mathbf{X}_i, f^{(s)}(\mathbf{X}_i); \boldsymbol{\theta}) \right) + \frac{1}{m} \sum_{j=1}^m l(\tilde{\mathbf{X}}_j, f^{(s)}(\tilde{\mathbf{X}}_j); \boldsymbol{\theta}) \\ & \xrightarrow{p} \mathbb{E}[l(\mathbf{X}_i, Y_i; \boldsymbol{\theta})] - \mathbb{E}[l(\mathbf{X}_i, f^{(s)}(\mathbf{X}_i); \boldsymbol{\theta})] + \mathbb{E}[l(\tilde{\mathbf{X}}_j, f^{(s)}(\tilde{\mathbf{X}}_j); \boldsymbol{\theta})] = \mathbb{E}[l(\mathbf{X}_i, Y_i; \boldsymbol{\theta})], \end{aligned}$$

where the equality is because \mathbf{X}_i from the small labeled dataset and $\tilde{\mathbf{X}}_j$ from the large unlabeled dataset are sampled from the same distribution. Since l has a unique minimizer, Theorem 2.7 of Newey and McFadden (1994) ensures that $\hat{\boldsymbol{\theta}}$ is consistent.

Because $\hat{\boldsymbol{\theta}}$ is consistent, we focus on the asymptotic covariance matrix of $\hat{\boldsymbol{\theta}}$. The asymptotic covariance matrix of $\hat{\boldsymbol{\theta}}$ is given by the sandwich variance formula.

LEMMA 1 (Angelopoulos et al. (2023b) Theorem 1). *The asymptotic variance of $\hat{\boldsymbol{\theta}}$ is*

$$\text{Var}(\hat{\boldsymbol{\theta}}) = \mathbf{H}^{-1} \mathbf{V} \mathbf{H}^{-1},$$

where

$$\begin{aligned} \mathbf{H} &= \mathbb{E}[\mathbf{H}_\theta l(\mathbf{X}, Y; \boldsymbol{\theta}^*)], \\ \mathbf{V} &= \frac{1}{n-s} \text{Var}(\psi(\mathbf{X}, Y; \boldsymbol{\theta}^*) - \psi(\mathbf{X}, f^{(s)}(\mathbf{X}); \boldsymbol{\theta}^*)) + \frac{1}{m} \text{Var}(\psi(\tilde{\mathbf{X}}, f^{(s)}(\tilde{\mathbf{X}}); \boldsymbol{\theta}^*)). \end{aligned}$$

Here, $\mathbf{H}_\theta l(\mathbf{X}, Y; \boldsymbol{\theta}^*)$ stands for the Hessian matrix of $l(\mathbf{X}, Y; \boldsymbol{\theta})$ evaluated at $\boldsymbol{\theta}^*$.

In the case when m is much larger than $n - s$, the second term can be ignored, and we focus our attention primarily on the first term. Note that the asymptotic variance of $\hat{\boldsymbol{\theta}}$ is a covariance matrix $\text{Var}(\hat{\boldsymbol{\theta}})$. To minimize the covariance matrix $\text{Var}(\hat{\boldsymbol{\theta}})$, a common strategy from the optimal experimental design literature is to scalarize it through various different objectives, and then minimize the scalarized objective (Atkinson et al. 2007, Fedorov 2013, Pukelsheim 2006, Silvey 2013). We discuss two objectives in this paper, including minimizing the determinant of the covariance matrix $\det(\text{Var}(\hat{\boldsymbol{\theta}}))$ and minimizing the trace of the covariance matrix $\text{tr}(\text{Var}(\hat{\boldsymbol{\theta}}))$, which correspond to the D-optimal and A-optimal objective, respectively. There are more objectives in the optimal experimental design literature; see Pukelsheim (2006), Atkinson et al. (2007), Fedorov (2013), Silvey (2013).

Determinant Minimization

We first consider minimizing the determinant of the covariance matrix $\det(\text{Var}(\hat{\boldsymbol{\theta}}))$. Intuitively, minimizing the determinant of the covariance matrix can be interpreted as minimizing the volume of the resulting confidence ellipsoid (Boyd and Vandenberghe 2004). Using the property that the determinant of a product of square matrices is equal to the product of their individual determinants, we have:

$$\det(\text{Var}(\hat{\boldsymbol{\theta}})) = \det(\mathbf{H}^{-1}) \frac{\det(\text{Var}(\boldsymbol{\psi}(\mathbf{X}, Y; \boldsymbol{\theta}^*) - \boldsymbol{\psi}(\mathbf{X}, f^{(s)}(\mathbf{X}); \boldsymbol{\theta}^*)))}{(n - s)^d} \det(\mathbf{H}^{-1}).$$

Because the Hessian term \mathbf{H} is a population quantity that does not depend on the fine-tuned function $f^{(s)}(\cdot)$, minimizing the total determinant is equivalent to minimizing the following objective function:

$$\frac{1}{(n - s)^d} \det(\text{Var}(\boldsymbol{\psi}(\mathbf{X}, Y; \boldsymbol{\theta}^*) - \boldsymbol{\psi}(\mathbf{X}, f^{(s)}(\mathbf{X}); \boldsymbol{\theta}^*))). \quad (8)$$

This objective function generalizes the objective function $\text{Var}(Y - f^{(s)}(\mathbf{X}))/(n - s)$ that we have considered in mean estimation. We denote the scalarized variance metric $\nu(s)$ as:

$$\nu(s) = \left[\det(\text{Var}(\boldsymbol{\psi}(\mathbf{X}, Y; \boldsymbol{\theta}^*) - \boldsymbol{\psi}(\mathbf{X}, f^{(s)}(\mathbf{X}); \boldsymbol{\theta}^*))) \right]^{1/d}.$$

The quantity $\nu(s)$ represents a “geometric average” variance per dimension. It is natural to model this scalar quantity using the power-law scaling relationship $\nu(s) = as^{-\alpha} + b$, where $\alpha, a > 0, b \geq 0$ are task-specific constants. When the constants are known, minimizing the determinant objective (8) is equivalent to solving the univariate optimization problem

$$\min_{s \in (0, n)} \frac{as^{-\alpha} + b}{n - s}.$$

This recovers the exact form of the optimization problem in (4). Consequently, all previous results, including Theorem 1 and Propositions 1–3, hold here.

Trace Minimization

Next, we consider minimizing the trace of the covariance matrix $\text{tr}(\text{Var}(\hat{\boldsymbol{\theta}}))$. Minimizing the trace of the covariance matrix corresponds to minimizing the mean-squared error of the estimator vector $E[\|\hat{\boldsymbol{\theta}} - \boldsymbol{\theta}^*\|_2^2]$ (Boyd and Vandenberghe 2004). Recall from Lemma 1 that the asymptotic covariance is $\mathbf{H}^{-1} \mathbf{V} \mathbf{H}^{-1}$. Using the cyclic property of the trace operator, we can express the total variance objective as:

$$\text{tr}(\text{Var}(\hat{\boldsymbol{\theta}})) = \text{tr}(\mathbf{H}^{-1} \mathbf{V} \mathbf{H}^{-1}) = \text{tr}((\mathbf{H}^{-1})^2 \mathbf{V}),$$

Because the Hessian term \mathbf{H} is a population quantity that does not depend on the fine-tuned function $f^{(s)}(\cdot)$, we can think of $(\mathbf{H}^{-1})^2$ as a fixed weighting matrix, and our objective is

$$\frac{1}{n-s} \text{tr}((\mathbf{H}^{-1})^2 \text{Var}(\boldsymbol{\psi}(\mathbf{X}, Y; \boldsymbol{\theta}^*) - \boldsymbol{\psi}(\mathbf{X}, f^{(s)}(\mathbf{X}); \boldsymbol{\theta}^*))). \quad (9)$$

We denote the numerator in (9) as the scalarized variance metric $\nu(s)$

$$\nu(s) = \text{tr}((\mathbf{H}^{-1})^2 \text{Var}(\boldsymbol{\psi}(\mathbf{X}, Y; \boldsymbol{\theta}^*) - \boldsymbol{\psi}(\mathbf{X}, f^{(s)}(\mathbf{X}); \boldsymbol{\theta}^*))).$$

The quantity $\nu(s)$ represents the mean-squared error of the estimator vector. It is natural to model this scalar quantity using same power-law scaling relationship $\nu(s) = as^{-\alpha} + b$, where $\alpha, a > 0, b \geq 0$ are task-specific constants. When the constants are known, minimizing the trace objective (9) is equivalent to solving the univariate optimization problem

$$\min_{s \in (0, n)} \frac{as^{-\alpha} + b}{n-s}.$$

This recovers the exact form of the optimization problem in (4). Consequently, all previous results, including Theorem 1 and Propositions 1–3, hold here.

Inference

Finally, we state the inference method provided by Angelopoulos et al. (2023b) to construct confidence intervals for M -estimation. We will make use of the prediction-powered M -estimator $\hat{\boldsymbol{\theta}}$ defined in (7). First, we estimate the sample covariance matrix

$$\hat{\mathbf{V}}_{f^{(s)}} = \frac{1}{m-1} \sum_{j=1}^m \left(\boldsymbol{\psi}(\mathbf{X}_j, f^{(s)}(\mathbf{X}_j); \hat{\boldsymbol{\theta}}) - \bar{\boldsymbol{\psi}} \right) \left(\boldsymbol{\psi}(\mathbf{X}_j, f^{(s)}(\mathbf{X}_j); \hat{\boldsymbol{\theta}}) - \bar{\boldsymbol{\psi}} \right)^\top$$

in the large unlabeled dataset, where $\bar{\boldsymbol{\psi}} = \frac{1}{m} \sum_{j=1}^m \boldsymbol{\psi}(\mathbf{X}_j, f^{(s)}(\mathbf{X}_j); \hat{\boldsymbol{\theta}})$. Second, we estimate the sample covariance matrix

$$\hat{\mathbf{V}}_{Y-f^{(s)}} = \frac{1}{n-s-1} \sum_{i=1}^{n-s} \left(\boldsymbol{\Delta}_i - \bar{\boldsymbol{\Delta}} \right) \left(\boldsymbol{\Delta}_i - \bar{\boldsymbol{\Delta}} \right)^\top$$

in the small labeled dataset, where $\Delta_i = \psi(\mathbf{X}_i, Y_i; \hat{\boldsymbol{\theta}}) - \psi(\mathbf{X}_i, f^{(s)}(\mathbf{X}_i); \hat{\boldsymbol{\theta}})$ and $\bar{\Delta} = \frac{1}{n-s} \sum_{i=1}^{n-s} \Delta_i$. Third, we estimate the sample Hessian matrix

$$\widehat{\mathbf{H}} = \frac{1}{n-s} \sum_{i=1}^{n-s} \mathbf{H}_{\boldsymbol{\theta}} l(\mathbf{X}_i, Y_i; \hat{\boldsymbol{\theta}})$$

in the labeled dataset. Finally, we calculate

$$\widehat{\boldsymbol{\Sigma}} = \widehat{\mathbf{H}}^{-1} \left(\frac{1}{n-s} \widehat{\mathbf{V}}_{Y-f^{(s)}} + \frac{1}{m} \widehat{\mathbf{V}}_{f^{(s)}} \right) \widehat{\mathbf{H}}^{-1}.$$

For any $\delta \in (0, 1)$ and any dimension $l \in [d]$, we calculate the following confidence interval

$$\left[\widehat{\theta}_l - z_{1-\frac{\delta}{2}} \sqrt{\widehat{\boldsymbol{\Sigma}}_{ll}}, \widehat{\theta}_l + z_{1-\frac{\delta}{2}} \sqrt{\widehat{\boldsymbol{\Sigma}}_{ll}} \right].$$

Theorem 1 of Angelopoulos et al. (2023b) suggests that the confidence interval constructed in this way is asymptotically valid.

6. Empirical Analysis

In this section, we present empirical evidence to validate our proposed framework. After introducing our empirical setup in Section 6.1, we conduct three empirical analyses. First, in Section 6.2, we assess the goodness-of-fit of the fine-tuning scaling law. Second, we test the optimal sample allocation rule in Section 6.3. Third, we compare our proposed method to several benchmarks in Section 6.4, highlighting the variance reduction and cost saving benefits of using the variance-based loss function in fine-tuning.

6.1. Empirical Setup

Textual product reviews are a common source of information for assessing perceived quality in many markets. Such reviews encode rich but noisy signals about latent product attributes that are difficult to measure directly. A central challenge for firms is to aggregate these textual evaluations into reliable quality measures.

This challenge is particularly important in settings where high-quality evaluations are costly. In such settings, each additional labeled observation is expensive, and improving statistical efficiency directly reduces the number of human evaluations needed to achieve a target level of precision. As a result, variance reduction is not only the technical goal; it has direct implications for how quickly and reliably firms can form aggregate assessments of product quality under fixed evaluation budgets.

Dataset and Estimand. We study this problem using the Wine Reviews dataset, consisting of wine reviews written by professional wine critics at *Wine Enthusiast* magazine and publicly available on Kaggle (Thoutt 2017). This dataset has also been used in prior work on prediction-powered inference and surrogate outcomes (Ji et al. 2025).

The dataset comprises 129,971 wine reviews, each containing a free-form natural language description of sensory characteristics, such as aroma, flavor, balance, and finish, alongside structured metadata. The outcome variable is an overall rating given by expert reviewers, ranging from 80 to 100 points (as the magazine only publishes reviews scoring above 80). This metric reflects a standardized professional rubric widely adopted in the industry. Two representative examples are provided in Table 1. After deleting the duplicated reviews, we have 119,955 unique reviews for our empirical analysis. Note that metadata is excluded from our analysis.

To get the population mean of ratings, we randomly partition the dataset into two disjoint sets: one with 109,955 unique reviews as the *target population*, another with 10,000 reviews to estimate the fine-tuning scaling law in Section 6.2. The population mean rating over the target population is 88.441, and is treated as the ground truth throughout the empirical analysis.

Table 1 Examples from the Wine Reviews dataset

Review (X)	This is a walk backward after the impressive 2012. Almost impenetrably black, the flavors converge around espresso and bitter chocolate, yet the tannins have a green edge. The wine simply feels flat in the mouth with no life to it.
Rating (Y)	85
Review (X)	This is one of the great Rieslings from the Wachau, a wonderful panoply of ripe, tropical fruit, pierced with flint, spice and minerality. It is rich and opulent, while never losing sight of the core tautness of a fine Riesling.
Rating (Y)	95

PPI Estimator Construction. In subsequent experiments in Section 6.3 and Section 6.4, for each independent replication and each budget setting with n labeled samples, we randomly draw n independent samples from the target population as the labeled dataset \mathcal{N} , part of which is used for LLM fine-tuning and the remaining for PPI rectification. All remaining reviews in the target population are treated as unlabeled data, denoted as \mathcal{M} , and are used for PPI estimator construction. Importantly, the 10,000 reviews used for scaling law estimation in Section 6.2 are never used in fine-tuning or PPI, ensuring a clean separation between scaling law estimation and downstream inference.

LLM Fine-Tuning. We treat the pretrained **Qwen3-Embedding-0.6B** model as the encoder h . Specifically, given an input text \mathbf{X} , we extract the final hidden layer to obtain a 1024-dimensional embedding, which is then passed through a small multilayer perceptron (MLP) regression head,

consisting of two linear layers with a ReLU activation, to produce the final surrogate prediction. To balance computational efficiency and task adaptation, we adopt a parameter-efficient fine-tuning strategy: we freeze the majority of the encoder parameters and jointly update only the last transformer layer of the encoder along with the MLP regression head. For each fine-tuning run, the available labeled data are randomly split into 80% for training and 20% for validation. The validation set is used exclusively for model selection, and the checkpoint achieving the best validation performance is retained for downstream inference.

Standard LLM fine-tuning for this type of rating typically minimizes MSE, which jointly penalizes both bias and variance. However, our objective is not prediction accuracy, but the efficient estimation of the population mean when there is a downstream PPI stage. In this setting, the residual variance of predictions is the primary determinant of statistical efficiency, as systematic bias can be subsequently corrected during the inference step using the remaining labeled data.

We fine-tune a model $f^{(s)}$ using a small subset of s samples from the labeled dataset \mathcal{N} . Model parameters are optimized via mini-batch stochastic gradient descent using the Adam optimizer. We adopt the residual variance-based regression objective discussed in Section 4.1, which directs the LLM to minimize the conditional spread of prediction errors. Specifically, for a mini-batch of size k , we compute the residuals $r_i = Y_i - f^{(s)}(\mathbf{X}_i)$ and their batch mean $\bar{r} = \frac{1}{k} \sum_{i=1}^k r_i$. The training loss is defined as the within-batch variance of these residuals $\mathcal{L}_{\text{var}} = \frac{1}{k} \sum_{i=1}^k (r_i - \bar{r})^2$.

6.2. Scaling Law Validation

Before evaluating the end-to-end performance of FT+PPI, we first empirically validate the scaling law behavior of our variance-based fine-tuning objective. This analysis is critical as it tests the fundamental assumption of power-law variance reduction,

$$\text{Var}\left(Y - f^{(s)}(\mathbf{X})\right) = as^{-\alpha} + b,$$

a relationship previously unexplored in the context of residual variance for LLM surrogates.

We randomly sample 10,000 labeled reviews, and randomly partition them into two subsets: 5,000 samples are used as a validation set, and the other 5,000 samples are used as training data during LLM fine-tuning. To validate the scaling law, we fine-tune a series of LLMs $f^{(s)}$ using varying training data size s out of the total 5,000 training samples. For each training data size s , the LLM is fine-tuned using the variance-based objective, and the resulting residual variance is evaluated on the shared validation set.

The results of this validation are presented in Figure 1, which shows the residual variance $\text{Var}(Y - f^{(s)}(\mathbf{X}))$ as a function of the fine-tuning subset size s . We also fit the parametric scaling law model to the data.

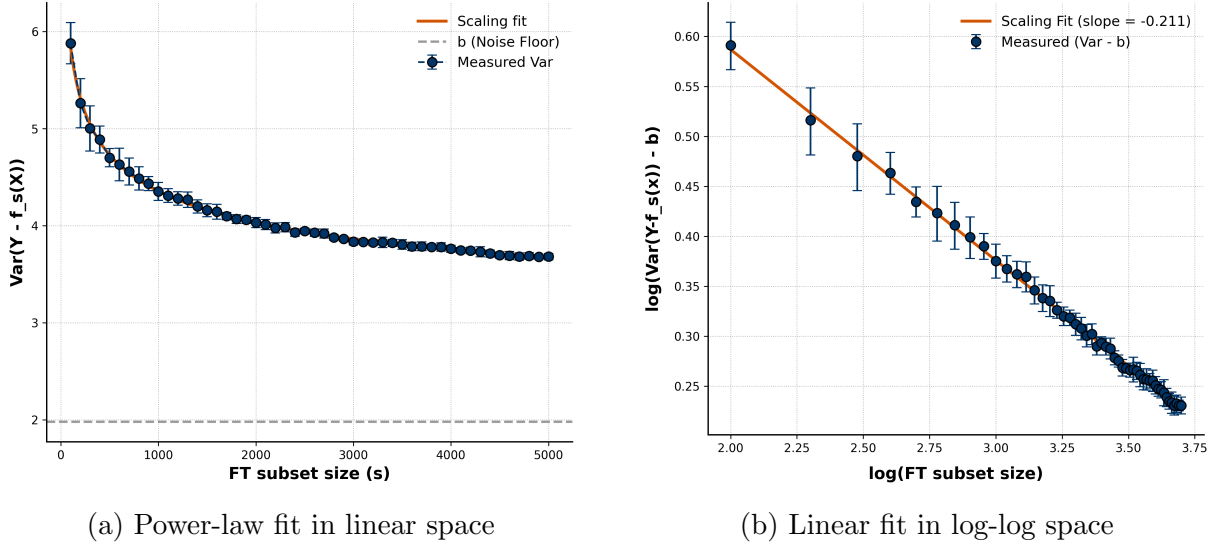


Figure 1 Empirical validation of the variance-based scaling law. The estimated parameters are $\hat{a} = 10.21$, $\hat{\alpha} = 0.21$, and $\hat{b} = 1.98$

The most striking finding is the exceptionally high goodness-of-fit, with an $R^2 = 0.998$. This confirms that the variance-based objective follows a highly predictable power-law decay, explaining nearly all of the observed variation in validation variance.

To further verify the robustness of these findings, we conducted extensive robustness checks detailed in Online Appendix EC.3.1. Using a bootstrap-based variance decomposition, we confirmed that the scaling law is a stable functional relationship that is robust to both training randomness (e.g., sample path, initialization, randomness of gradient descent, etc) and randomness of the training dataset. Specifically, while parameter estimates $(\hat{a}, \hat{\alpha}, \hat{b})$ may exhibit small dispersion across replicates, the implied optimal allocation ratio s^*/n remains remarkably concentrated, providing a reliable foundation for our data-driven allocation strategy.

6.3. Optimal Allocation of Labeled Samples

Next, we empirically evaluate the impact of sample allocation on estimation efficiency. Our primary goal is to validate that the allocation trade-off follows the predicted pattern and that our theoretical optimal allocation rule (Theorem 1) accurately identifies the empirical minimizer. We utilize the scaling law parameters $(\hat{a}, \hat{\alpha}, \hat{b}) = (10.21, 0.21, 1.98)$ estimated above as fixed inputs to derive the theoretical optimal allocation s^* , which is then tested against empirical performance.

We consider an inference setting where $n = 10000$ labeled samples are observed to construct the mean rating estimators. Using this labeled dataset \mathcal{N} , we vary the allocation fraction $s/n \in \{0\%, 5\%, 10\%, \dots, 95\%\}$ assigned to fine-tuning, while reserving the remaining $n - s$ labeled samples for PPI rectification. For each allocation ratio, we conduct 20 independent replications of the full fine-tuning and rectification pipeline to report the resulting confidence intervals. Note that, in each

replication, a labeled dataset \mathcal{N} of size n is randomly drawn from the target population. All reviews from the target population that are not selected into \mathcal{N} are treated as unlabeled data \mathcal{M} .

The results are shown in Figure 2, which presents a side-by-side comparison of the FT+PPI estimator using the standard MSE-based objective versus our proposed variance-based fine-tuning objective. 95% confidence intervals of the population mean estimators across repeated experiments are also displayed. For reference, we also report the sample mean estimator based on all labeled samples in \mathcal{N} , and this sample mean estimator is invariant to s/n .

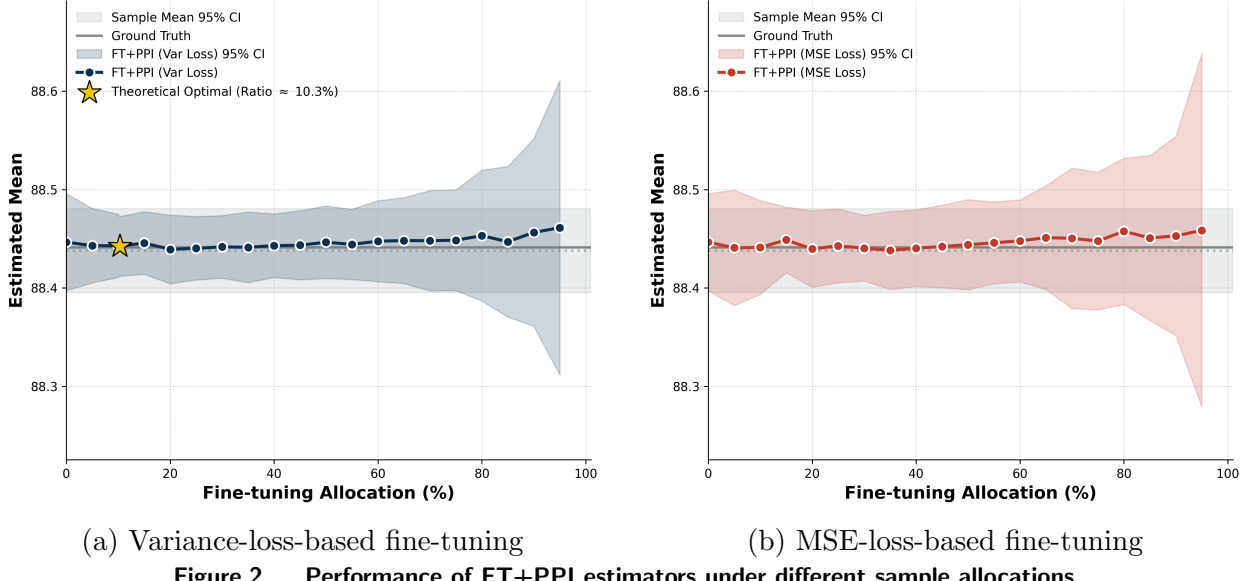


Figure 2 Performance of FT+PPI estimators under different sample allocations

First, Figure 2a confirms that the theoretically optimal allocation ratio $s^*/n \approx 10.3\%$ closely matches the empirical optimum, which lies around 10% (evaluated at 5% increments). In this region, the estimator achieves the narrowest confidence intervals, corresponding to the highest statistical efficiency. This observation empirically validates Theorem 1 and demonstrates the practical utility of our proposed variance-based scaling law. We also note that although this specific experiment does not strictly follow the iterative ramp-up procedure outlined in Online Appendix EC.2, similar results are achievable if using the ramp-up procedure; as indicated by the scaling law fit in Figure 1, accurate scaling law estimates can be obtained with a small subset of approximately 1,000 labeled samples.

Second, we observe a decreasing-then-increasing pattern in confidence interval widths as the fine-tuning sample proportion s/n increases. This trend empirically confirms the trade-off between fine-tuning quality and PPI rectification precision analytically discussed in Section 4.1. However, the variance-based fine-tuning yields uniformly tighter confidence intervals across all allocation

regimes. This confirms that the superior reduction in residual variance observed in Figure EC.3 directly translates into more efficient downstream inference.

Third, we analyze the conditions under which FT+PPI outperforms the SAMPLE MEAN estimator. Recall Proposition 2, which establishes that FT+PPI improves upon the SAMPLE MEAN whenever the predictive $R^2(s) = 1 - \text{Var}(Y - f^{(s)}(\mathbf{X}))/\text{Var}(Y)$ of the fine-tuned model exceeds the fraction of labeled data consumed by fine-tuning, s/n .

Figure 3 plots the measure, $R^2(s) - s/n$, as a function of the allocation ratio s/n . The result matches our previous findings in Figure 2a.

- Region of Improvement: The gain is positive for allocation ratios between 0% and approx. 60%. In this regime, the variance reduction from the surrogate model outweighs the data cost, meaning FT+PPI statistically dominates the SAMPLE MEAN.
- Optimal Peak: The curve exhibits a distinct inverted U-shape, rising sharply to peak at approximately 10%. This maximum corresponds exactly to the “sweet spot” of highest efficiency (narrowest confidence intervals) identified earlier.
- Diminishing Returns: Beyond this peak, the efficiency gain declines as the linear penalty of data consumption (s/n) begins to overwhelm the diminishing marginal returns of the fine-tuning scaling law, eventually turning negative beyond 60%.

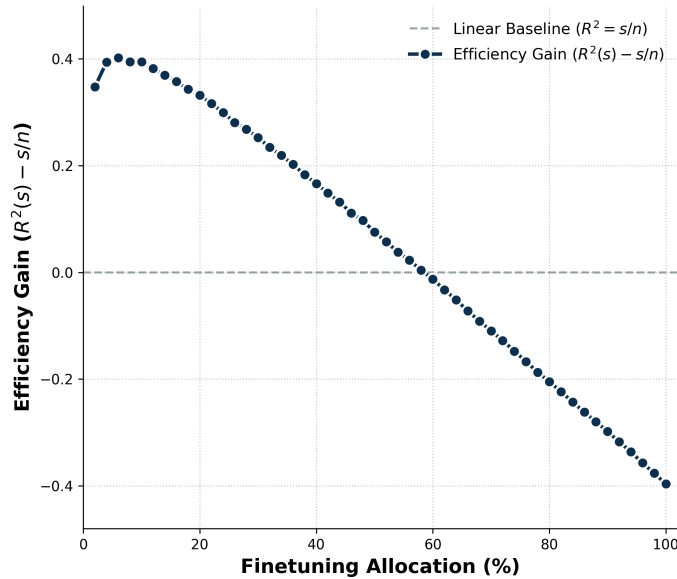


Figure 3 Efficiency gain ($R^2(s) - s/n$) from fine-tuning allocation. Positive values indicate regions where FT+PPI outperforms the Sample Mean Estimator.

6.4. Comparison of Different Estimators

We evaluate the performance of our proposed framework against standard benchmarks across varying labeled data budgets, $n \in \{1000, 3000, 5000, 10000\}$. This range allows us to assess the method’s effectiveness in both data-scarce and data-rich regimes.

We compare the following five estimators:

- **SAMPLE MEAN:** The classical unbiased estimator averaging over n labeled samples.
- **FT-ONLY:** A model fine-tuned on all n samples using standard MSE loss. No PPI rectification is applied; estimates are generated by averaging the fine-tuned LLM surrogates. Note that this is the only biased estimator among the five compared estimators.
- **PPI-ONLY (Few-shot Prompting):** This estimator uses the off-the-shelf base LLM without any fine-tuning. Because the base LLM does not include a trained regression head, we elicit ratings via few-shot prompting; the full prompt is provided in Online Appendix EC.3.2. In contrast, all estimators involving fine-tuning use the learned regression head and do not rely on prompting.
- **FT+PPI (MSE Loss):** A hybrid approach where the model is fine-tuned with MSE loss on a subset of data, and the remaining data is used for PPI. As there is no theoretical alignment between the MSE objective and PPI variance reduction, we perform a grid search over allocation ratios (at 5% intervals) and report the empirically best-performing result.
- **FT+PPI (VAR Loss):** Our proposed method. The model is fine-tuned using the variance-based objective, and samples are split according to the theoretically optimal allocation ratio s^*/n .

Estimation Accuracy. Table 2 reports the Root Mean Squared Error (RMSE), Mean Absolute Error (MAE), and Mean Absolute Percentage Error (MAPE) for the population mean estimate. We discuss two major observations in the following.

First, FT-ONLY consistently performs the worst across all budget settings, particularly as n increases. This underperformance arises because FT-ONLY remains a biased estimator even with large n , and the marginal benefit of additional fine-tuning data diminishes more quickly than other estimators according to a scaling law (typically with $\alpha < 1$). This highlights a critical managerial risk: deploying fine-tuned models directly for measurement without rectification can lead to significant bias.

Second, our proposed FT+PPI (VAR Loss) achieves the highest accuracy across all metrics and budget levels, outperforming all other benchmarks, particularly the FT+PPI (MSE Loss) variant. This validates our core theoretical insight: minimizing residual variance rather than MSE is the optimal objective for downstream rectification. To better understand the mechanism behind this performance gain, we analyze the residual variance achieved by the two objectives in Online Appendix EC.3.3. We find that the variance-based objective consistently yields lower residual variance than the MSE objective, particularly in the low-sample regime. This confirms that decoupling

Table 2 Estimation accuracy across estimators under different labeled sample sizes n

n	Estimator	RMSE ($\times 10^{-2}$)	MAE ($\times 10^{-2}$)	MAPE ($\times 10^{-2}\%$)
1000	SAMPLE MEAN	11.01 (1.80)	8.695 (1.495)	9.831 (1.706)
	FT-ONLY	12.02 (1.64)	9.414 (1.672)	10.64 (1.89)
	PPI-ONLY	9.121 (1.426)	7.132 (1.270)	8.065 (1.439)
	FT+PPI (MSE Loss)	9.354 (1.347)	7.467 (1.256)	8.443 (1.435)
	FT+PPI (VAR Loss)	6.713 (0.729)	5.527 (0.846)	6.249 (0.967)
3000	SAMPLE MEAN	5.315 (1.027)	3.817 (0.827)	4.316 (0.944)
	FT-ONLY	8.050 (0.920)	6.807 (0.969)	7.697 (1.065)
	PPI-ONLY	4.094 (0.540)	3.334 (0.534)	3.769 (0.611)
	FT+PPI (MSE Loss)	3.947 (0.574)	3.301 (0.484)	3.732 (0.542)
	FT+PPI (VAR Loss)	3.583 (0.548)	2.801 (0.495)	3.167 (0.561)
5000	SAMPLE MEAN	4.486 (0.750)	3.557 (0.617)	4.022 (0.689)
	FT-ONLY	8.913 (0.878)	7.799 (0.973)	8.819 (1.081)
	PPI-ONLY	4.889 (0.541)	4.221 (0.566)	4.772 (0.640)
	FT+PPI (MSE Loss)	4.151 (0.673)	3.224 (0.586)	3.645 (0.667)
	FT+PPI (VAR Loss)	3.291 (0.444)	2.670 (0.430)	3.019 (0.475)
10000	SAMPLE MEAN	2.199 (0.306)	1.874 (0.261)	2.119 (0.290)
	FT-ONLY	5.068 (0.715)	4.013 (0.692)	4.537 (0.782)
	PPI-ONLY	2.504 (0.397)	2.004 (0.335)	2.266 (0.379)
	FT+PPI (MSE Loss)	1.662 (0.224)	1.362 (0.210)	1.540 (0.243)
	FT+PPI (VAR Loss)	1.470 (0.230)	1.103 (0.221)	1.247 (0.238)

Note: Reported values are averages across 20 independent experiment replications. Numbers in parentheses denote standard errors (SE). All error metrics are reported after applying the scale factors indicated in the column headers. For each n , the best-performing estimator (lowest error) is highlighted in bold.

variance reduction from bias correction and leaving the latter to the PPI stage is the effective driver of the improved downstream efficiency observed here.

Sample Savings. To quantify the business value of our framework, we analyze two equivalent metrics: *variance reduction* and *sample savings*. We define *variance reduction* as the percentage decrease in the estimator’s variance relative to the baseline SAMPLE MEAN. We translate this statistical metric into *sample savings* to quantify the tangible economic benefit of reducing labeled data acquisition costs.

Specifically, let n be the actual sample size used by our estimator, and let n_{equiv} be the equivalent sample size required by the SAMPLE MEAN to match our estimator’s variance. Because the variance of the SAMPLE MEAN scales inversely with sample size (i.e., $\text{Var} \propto 1/n$), the ratio of variances is exactly the inverse ratio of the effective sample sizes: $\text{Var}(\hat{\mu}_{\text{FT+PPI}})/\text{Var}(\hat{\mu}_{\text{SAMPLE MEAN}}) = n/n_{\text{equiv}}$. Consequently, the sample saving metric, defined as $1 - n/n_{\text{equiv}}$, is mathematically identical to the variance reduction, $1 - \text{Var}(\hat{\mu}_{\text{FT+PPI}})/\text{Var}(\hat{\mu}_{\text{SAMPLE MEAN}})$. Table 3 presents these results.

The economic benefits are substantial. Across all labeled data budgets, our variance-optimized framework delivers sizable efficiency gains, with sample savings ranging from approximately 45% to 66% compared to SAMPLE MEAN. For instance, when $n = 10000$, FT+PPI (VAR Loss) achieves a variance reduction of 54.71% relative to the SAMPLE MEAN. Practically, this implies that a market

Table 3 Variance Reduction and Sample Savings w.r.t. Sample Mean

n	FT+PPI (Var Loss) vs. SAMPLE MEAN		FT+PPI (MSE Loss) vs. SAMPLE MEAN		FT+PPI: Var vs. MSE Loss
	Variance Reduction (%)	Sample Savings (%)	Variance Reduction (%)	Sample Savings (%)	Variance Reduction (%)
1000	66.09 (15.56)	66.09 (15.56)	25.60 (34.14)	25.60 (34.14)	54.43 (20.91)
3000	54.66 (20.80)	54.66 (20.80)	44.83 (25.32)	44.83 (25.32)	17.83 (37.70)
5000	45.51 (25.00)	45.51 (25.00)	13.75 (39.57)	13.75 (39.57)	36.82 (28.99)
10000	54.71 (20.78)	54.71 (20.78)	41.56 (26.81)	41.56 (26.81)	22.50 (35.56)

Note: Reported values are averages across 20 independent experiment replications. Sample savings are computed under the assumption that estimator variance scales inversely with the labeled sample size, and therefore numerically coincide with variance reduction.

research team can attain comparable statistical accuracy while labeling only half the data, leading to substantial cost reductions. Alternatively, for a fixed labeling budget, the same team can obtain markedly tighter confidence intervals, enabling more precise downstream decisions.

The comparison with FT+PPI (MSE Loss) further highlights a nontrivial limitation of the standard fine-tuning practice. Although MSE-based fine-tuning combined with PPI improves upon the SAMPLE MEAN, its efficiency gains are systematically smaller than those achieved by variance-based fine-tuning. For example, at $n = 1000$, FT+PPI (VAR Loss) yields a 66.09% variance reduction, compared to only 25.60% for its MSE-based counterpart. This gap persists across all budget settings of n . The last column of Table 3 reports the variance reductions of 18%–54% when replacing the MSE objective with the variance-based objective. These results underscore our core message: optimizing the LLM surrogate for residual variance, rather than predictive accuracy, is critical for achieving efficient downstream inference.

7. Conclusions

In this paper, we propose a fine-tuning then rectification framework for leveraging LLMs as human surrogates under limited human labeled data. We show that the statistical efficiency of the downstream rectification estimator is governed primarily by the residual variance of the LLM surrogates. Consequently, we propose a variance-based fine-tuning objective that outperforms the standard fine-tuning objective of mean-squared error. Furthermore, we leverage empirical scaling laws to derive a data-driven procedure for optimally allocating scarce labeled samples between fine-tuning and rectification. Empirical results confirm that our fine-tuning then rectification framework outperforms using either fine-tuning or rectification alone, as well as using the standard fine-tuning objective of mean-squared error. Empirical results also confirm that our theoretically derived allocation closely matches the empirical optimum.

We view this work as an initial step toward a systematic understanding of how to jointly optimize LLM model improvement and statistical correction. In this work, we have also provided practical ready-to-use solutions for two important implementation approaches: estimating scaling

law parameters via a ramp-up procedure (see Online Appendix EC.2) and handling independent but non-identical fine-tuning data (see Online Appendix EC.4). These approaches are sometimes effective in practice, and offer fertile grounds for future research. For instance, we currently model the non-identical setting simply through changes in scaling law parameters, yet more theoretical and empirical analysis of such transfer-learning dynamics remains to be explored. Similarly, the optimality of the data-driven ramp-up strategy could be further investigated. As LLMs become increasingly integrated into market research and social science applications, developing such rigorous methodologies for combining residual variance reduction (via fine-tuning) with bias correction (via rectification) will be essential for conducting surveys at scale.

Acknowledgments

The authors would like to thank Lihua Lei and Ruohan Zhan for their insightful comments that have greatly improved this paper.

References

Alfaro JA, Corbett CJ (2003) The value of sku rationalization in practice (the pooling effect under suboptimal inventory policies and nonnormal demand). *Production and Operations Management* 12(1):12–29.

Angelopoulos AN, Bates S, Fannjiang C, Jordan MI, Zrnic T (2023a) Prediction-powered inference. *Science* 382(6671):669–674.

Angelopoulos AN, Duchi JC, Zrnic T (2023b) PPI++: Efficient prediction-powered inference. *arXiv preprint arXiv:2311.01453* .

Argyle LP, Busby EC, Fulda N, Gubler JR, Rytting C, Wingate D (2023) Out of one, many: Using language models to simulate human samples. *Political Analysis* 31(3):337–351.

Atkinson A, Donev A, Tobias R (2007) *Optimum experimental designs, with SAS*, volume 34 (OUP Oxford).

Berry S, Levinsohn J, Pakes A (1995) Automobile prices in market equilibrium. *Econometrica* 63(4):841–890.

Boyd S, Vandenberghe L (2004) *Convex optimization* (Cambridge university press).

Brand J, Israeli A, Ngwe D (2023) Using LLMs for market research. *Harvard business school marketing unit working paper* (23-062).

Brown T, Mann B, Ryder N, Subbiah M, Kaplan JD, Dhariwal P, Neelakantan A, Shyam P, Sastry G, Askell A, et al. (2020) Language models are few-shot learners. *Advances in neural information processing systems* 33:1877–1901.

Brucks M, Toubia O (2023) Prompt architecture can induce methodological artifacts in large language models. *Available at SSRN 4484416* .

Cheng M, Ofek E, Yoganarasimhan H (2025) Balancing engagement and polarization: Multi-objective alignment of news content using LLMs. *arXiv preprint arXiv:2504.13444* .

Elmachtoub AN, Grigas P (2022) Smart “predict, then optimize”. *Management Science* 68(1):9–26.

Fedorov VV (2013) *Theory of optimal experiments* (Elsevier).

Ferreira KJ, Lee BHA, Simchi-Levi D (2016) Analytics for an online retailer: Demand forecasting and price optimization. *Manufacturing & service operations management* 18(1):69–88.

Gallego G, Topaloglu H, et al. (2019) *Revenue management and pricing analytics*, volume 209 (Springer).

Green PE, Srinivasan V (1990) Conjoint analysis in marketing: new developments with implications for research and practice. *Journal of marketing* 54(4):3–19.

Gui G, Toubia O (2023) The challenge of using LLMs to simulate human behavior: A causal inference perspective. *arXiv preprint arXiv:2312.15524* .

Han Z, Gao C, Liu J, Zhang J, Zhang SQ (2024) Parameter-efficient fine-tuning for large models: A comprehensive survey. *arXiv preprint arXiv:2403.14608* .

Hernandez D, Kaplan J, Henighan T, McCandlish S (2021) Scaling laws for transfer. *arXiv preprint arXiv:2102.01293* .

Hoffmann J, Borgeaud S, Mensch A, Buchatskaya E, Cai T, Rutherford E, Casas DdL, Hendricks LA, Welbl J, Clark A, et al. (2022) Training compute-optimal large language models. *arXiv preprint arXiv:2203.15556* .

Hu EJ, Shen Y, Wallis P, Allen-Zhu Z, Li Y, Wang S, Wang L, Chen W, et al. (2022) Lora: Low-rank adaptation of large language models. *ICLR* 1(2):3.

Ji W, Lei L, Zrnic T (2025) Predictions as surrogates: Revisiting surrogate outcomes in the age of ai. *arXiv preprint arXiv:2501.09731* .

Kaplan J, McCandlish S, Henighan T, Brown TB, Chess B, Child R, Gray S, Radford A, Wu J, Amodei D (2020) Scaling laws for neural language models. *arXiv preprint arXiv:2001.08361* .

Krsteski S, Russo G, Chang S, West R, Gligorić K (2025) Valid survey simulations with limited human data: The roles of prompting, fine-tuning, and rectification. *arXiv preprint arXiv:2510.11408* .

Lee HL, Billington C, Carter B (1993) Hewlett-packard gains control of inventory and service through design for localization. *Interfaces* 23(4):1–11.

Lee HL, Tang CS (1997) Modelling the costs and benefits of delayed product differentiation. *Management science* 43(1):40–53.

Li A, Chen H, Namkoong H, Peng T (2025) LLM generated persona is a promise with a catch. *arXiv preprint arXiv:2503.16527* .

Li P, Castelo N, Katona Z, Sarvary M (2024) Frontiers: Determining the validity of large language models for automated perceptual analysis. *Marketing Science* 43(2):254–266.

Motoki F, Pinho Neto V, Rodrigues V (2024) More human than human: measuring chatgpt political bias. *Public Choice* 198(1):3–23.

Newey WK, McFadden D (1994) Large sample estimation and hypothesis testing. *Handbook of econometrics* 4:2111–2245.

OpenAI (2025) Introducing gpt-oss. URL <https://openai.com/index/introducing-gpt-oss/>, accessed: 2025-12.

Ouyang L, Wu J, Jiang X, Almeida D, Wainwright C, Mishkin P, Zhang C, Agarwal S, Slama K, Ray A, et al. (2022) Training language models to follow instructions with human feedback. *Advances in neural information processing systems* 35:27730–27744.

Peng T, Gui G, Merlau DJ, Fan GJ, Sliman MB, Brucks M, Johnson EJ, Morwitz V, Althenayyan A, Bellezza S, et al. (2025) A mega-study of digital twins reveals strengths, weaknesses and opportunities for further improvement. *arXiv preprint arXiv:2509.19088* .

Pezeshkpour P, Hruschka E (2024) Large language models sensitivity to the order of options in multiple-choice questions. *Findings of the Association for Computational Linguistics: NAACL 2024*, 2006–2017.

Pukelsheim F (2006) *Optimal design of experiments* (SIAM).

Rafailov R, Sharma A, Mitchell E, Manning CD, Ermon S, Finn C (2023) Direct preference optimization: Your language model is secretly a reward model. *Advances in neural information processing systems* 36:53728–53741.

Silvey S (2013) *Optimal design: an introduction to the theory for parameter estimation*, volume 1 (Springer Science & Business Media).

Talluri KT, Van Ryzin GJ (2006) *The theory and practice of revenue management*, volume 68 (Springer Science & Business Media).

Thoutt Z (2017) Wine review dataset. Kaggle dataset, URL <https://www.kaggle.com/datasets/zyncide/wine-reviews/data>, accessed: 2025-12.

Tirole J (1988) *The theory of industrial organization* (MIT press).

Toubia O, Gui GZ, Peng T, Merlau DJ, Li A, Chen H (2025) Database report: Twin-2k-500: A data set for building digital twins of over 2,000 people based on their answers to over 500 questions. *Marketing Science* 44(6):1446–1455.

Vafa K, Athey S, Blei DM (2025) Estimating wage disparities using foundation models. *Proceedings of the National Academy of Sciences* 122(22):e2427298122.

Wang M, Zhang DJ, Zhang H (2024) Large language models for market research: A data-augmentation approach. *arXiv preprint arXiv:2412.19363* .

Wei J, Wang X, Schuurmans D, Bosma M, Xia F, Chi E, Le QV, Zhou D, et al. (2022) Chain-of-thought prompting elicits reasoning in large language models. *Advances in neural information processing systems* 35:24824–24837.

Wertenbroch K, Skiera B (2002) Measuring consumers' willingness to pay at the point of purchase. *Journal of marketing research* 39(2):228–241.

Wind J, Mahajan V (1997) Issues and opportunities in new product development: An introduction to the special issue. *Journal of marketing research* 34(1):1–12.

Ye Z, Yoganarasimhan H, Zheng Y (2025) LOLA: LLM-assisted online learning algorithm for content experiments. *Marketing Science* 44(5):995–1016.

Zhang B, Liu Z, Cherry C, Firat O (2024) When scaling meets llm finetuning: The effect of data, model and finetuning method. *arXiv preprint arXiv:2402.17193* .

Ziems C, Held W, Shaikh O, Chen J, Zhang Z, Yang D (2024) Can large language models transform computational social science? *Computational Linguistics* 50(1):237–291.

Online Appendix

EC.1. Missing Proofs

Proof of Theorem 1

Proof of Theorem 1. We consider the optimization problem as in (3). Denote

$$V(s) = \frac{as^{-\alpha} + b}{n - s}.$$

We then find the first order derivative,

$$\begin{aligned} V'(s) &= \frac{-\alpha as^{-\alpha-1}(n-s) + (as^{-\alpha} + b)}{(n-s)^2} \\ &= \frac{-\alpha ans^{-\alpha-1} + (\alpha+1)as^{-\alpha} + b}{(n-s)^2}. \end{aligned}$$

Setting $V'(s) = 0$, we have

$$\alpha ans^{-\alpha-1} - (\alpha+1)as^{-\alpha} - b = 0. \quad (\text{Eq.1})$$

Let $h(s) = \alpha ans^{-\alpha-1} - (\alpha+1)as^{-\alpha}$. Then we know $h'(s) = -\alpha(\alpha+1)\left(\frac{n}{s}-1\right)as^{-\alpha-1} < 0$. This means that the left-hand side of (Eq.1) is monotone decreasing. Note that, when $s \rightarrow 0^+$, the left-hand side of (Eq.1) can be expressed as $as^{-\alpha}\left(\frac{\alpha n}{s} - \alpha - 1\right) - b \rightarrow +\infty$. When $s = n$, the left-hand side of (Eq.1) can be expressed as $-an^{-\alpha} - b < 0$. So there exists a unique solution s^* between 0 and n that solves equation (Eq.1).

□

Proof of Proposition 1

Proof of Proposition 1. For clarity, write $s^* = s^*(a, b, \alpha, n)$ for the unique solution in $(0, n)$ to

$$F(s; a, b, \alpha, n) := \alpha ans^{-\alpha-1} - (\alpha+1)as^{-\alpha} - b = 0, \quad (\text{Eq.2})$$

where $a > 0$, $b \geq 0$, $\alpha > 0$, and $n > 0$. Differentiating with respect to s , we have,

$$\frac{\partial F}{\partial s} = a\alpha(\alpha+1)s^{-\alpha-2}(s-n) < 0 \quad \text{for all } s \in (0, n),$$

so $F(\cdot)$ is strictly decreasing and s^* is well-defined and unique.

Rewriting the first-order condition (Eq.2) gives

$$\alpha n = (\alpha+1)s^* + \frac{b}{a}(s^*)^{\alpha+1}, \quad \text{equivalently} \quad n = \frac{\alpha+1}{\alpha}s^* + \frac{b}{a\alpha}(s^*)^{\alpha+1}. \quad (\text{Eq.3})$$

Differentiate F with respect to a , b , and n :

$$\frac{\partial F}{\partial a} = \alpha ns^{-\alpha-1} - (\alpha+1)s^{-\alpha}, \quad \frac{\partial F}{\partial b} = -1, \quad \frac{\partial F}{\partial n} = \alpha as^{-\alpha-1}.$$

At $s = s^*$, use $F(s^*; a, b, \alpha, n) = 0$ to rewrite

$$b = \alpha a n(s^*)^{-\alpha-1} - (\alpha + 1) a(s^*)^{-\alpha} = a \frac{\partial F}{\partial a}(s^*),$$

so $\partial F/\partial a(s^*) = b/a \geq 0$.

By the implicit function theorem, for any parameter $\theta \in \{a, b, n\}$,

$$\frac{\partial s^*}{\partial \theta} = -\left. \frac{\partial F/\partial \theta}{\partial F/\partial s} \right|_{s=s^*}.$$

Since $\partial F/\partial s < 0$ on $(0, n)$, we obtain:

(i) *Dependence on a.*

$$\frac{\partial s^*}{\partial a} = -\frac{(b/a)}{\partial F/\partial s} \begin{cases} > 0, & b > 0, \\ = 0, & b = 0, \end{cases}$$

so s^* is nondecreasing in a and strictly increasing when $b > 0$. The same sign carries over to s^*/n since n is fixed in this derivative.

(ii) *Dependence on b.*

$$\frac{\partial s^*}{\partial b} = -\frac{-1}{\partial F/\partial s} = \frac{1}{\partial F/\partial s} < 0,$$

so s^* and s^*/n are strictly decreasing in b .

(iii) *Dependence on n.*

$$\frac{\partial s^*}{\partial n} = -\frac{\alpha a(s^*)^{-\alpha-1}}{\partial F/\partial s} > 0,$$

so s^* is strictly increasing in n .

(iv) *Dependence of s^*/n on n.* Starting from (Eq.3), write

$$n = c_1 s^* + c_2 (s^*)^{\alpha+1}, \quad c_1 := \frac{\alpha+1}{\alpha} > 0, \quad c_2 := \frac{b}{a\alpha} \geq 0.$$

Differentiate both sides with respect to n (treating $s^* = s^*(n)$):

$$1 = (c_1 + c_2(\alpha+1)(s^*)^\alpha) \frac{ds^*}{dn},$$

so

$$\frac{ds^*}{dn} = \frac{1}{c_1 + c_2(\alpha+1)(s^*)^\alpha} = \frac{a\alpha}{(a + b(s^*)^\alpha)(\alpha+1)}.$$

Now

$$\frac{d}{dn} \left(\frac{s^*}{n} \right) = \frac{n ds^*/dn - s^*}{n^2}.$$

Using $n = c_1 s^* + c_2 (s^*)^{\alpha+1}$ from (Eq.3), a short calculation yields

$$n \frac{ds^*}{dn} - s^* = -\frac{\alpha b (s^*)^{\alpha+1}}{(a + b(s^*)^\alpha)(\alpha+1)}.$$

Therefore, for $b > 0$,

$$\frac{d}{dn} \left(\frac{s^*}{n} \right) = -\frac{\alpha b (s^*)^{\alpha+1}}{n^2(a+b(s^*)^\alpha)(\alpha+1)} < 0,$$

so s^*/n is strictly decreasing in n .

Moreover, since $a + b(s^*)^\alpha \geq a$ and $s^* < n$, we bound

$$\left| \frac{d}{dn} \left(\frac{s^*}{n} \right) \right| \leq \frac{\alpha b (s^*)^{\alpha+1}}{n^2 a (\alpha+1)} \leq \frac{\alpha b}{\alpha+1} \frac{n^{\alpha+1}}{n^2 a} = \frac{\alpha}{\alpha+1} \frac{b}{a} n^{\alpha-1},$$

which is (5).

Finally, we consider the limit as $n \rightarrow \infty$ for $b > 0$. Dividing (Eq.3) by n gives

$$1 = \frac{\alpha+1}{\alpha} \frac{s^*}{n} + \frac{b}{a\alpha} \frac{(s^*)^{\alpha+1}}{n}.$$

Let $L = \lim_{n \rightarrow \infty} s^*/n$. Since $s^*/n \in (0, 1)$, L must be finite. Suppose for the sake of contradiction that $L > 0$. Then as $n \rightarrow \infty$, $s^* \rightarrow \infty$ linearly with n . The term $\frac{(s^*)^{\alpha+1}}{n} = \frac{s^*}{n} (s^*)^\alpha$ behaves like $L \cdot (Ln)^\alpha$, which tends to ∞ (since $\alpha > 0$). This implies the right-hand side of the equation diverges to infinity while the left-hand side is fixed at 1, a contradiction. Thus, we must have $L = 0$, i.e., $\lim_{n \rightarrow \infty} s^*/n = 0$.

(v) *Special case $b = 0$* . If $b = 0$, (Eq.3) simplifies to

$$\alpha n = (\alpha+1)s^* \Rightarrow \frac{s^*}{n} = \frac{\alpha}{\alpha+1},$$

which is exactly constant in a and n . □

Proof of Proposition 2

Proof of Proposition 2. Under the infinite- m approximation, the variance of the estimator is

$$\text{Var}(\hat{\mu}) = \frac{1}{n-s} \text{Var}(Y - f^{(s)}(\mathbf{X})).$$

Comparing this to the variance of the sample mean:

$$\text{Var}(\hat{\mu}) < \text{Var}(\hat{\mu}_{\text{mean}}) \iff \frac{\text{Var}(Y - f^{(s)}(\mathbf{X}))}{n-s} < \frac{\text{Var}(Y)}{n}.$$

Multiplying both sides by $(n-s)/\text{Var}(Y)$ (noting $n-s > 0$) yields

$$\frac{\text{Var}(Y - f^{(s)}(\mathbf{X}))}{\text{Var}(Y)} < \frac{n-s}{n} = 1 - \frac{s}{n}.$$

Recalling the definition $1 - R^2(s) = \text{Var}(Y - f^{(s)}(\mathbf{X}))/\text{Var}(Y)$, the inequality becomes

$$1 - R^2(s) < 1 - \frac{s}{n} \iff R^2(s) > \frac{s}{n}.$$

□

Proof of Proposition 3

Proof of Proposition 3. (i) Under the asymptotic assumption ($m \rightarrow \infty$), we have $\text{Var}(\hat{\mu}_{\text{FT+PPI}}) = (as^{-\alpha} + b)/(n - s)$. The condition $\text{Var}(\hat{\mu}_{\text{FT+PPI}}) < \text{Var}(\hat{\mu}_{\text{mean}})$ is equivalent to

$$\frac{as^{-\alpha} + b}{n - s} < \frac{\sigma^2}{n} \iff n(as^{-\alpha} + b) < \sigma^2(n - s) \iff q(s) > 0.$$

Thus, an improvement exists if and only if the maximum of $q(s)$ over the interval $(0, n)$ is positive.

(ii) To derive the explicit condition, we analyze the extrema of $q(s)$. Differentiating $q(s)$ with respect to s :

$$q'(s) = -\sigma^2 + a\alpha ns^{-\alpha-1}, \quad q''(s) = -a\alpha(\alpha+1)ns^{-\alpha-2}.$$

Since $a, \alpha, n, s > 0$, we have $q''(s) < 0$ for all $s > 0$, implying $q(s)$ is strictly concave. The unique unconstrained maximizer s_0 is found by setting $q'(s) = 0$:

$$a\alpha ns^{-\alpha-1} = \sigma^2 \implies s_0 = \left(\frac{a\alpha n}{\sigma^2}\right)^{1/(\alpha+1)}.$$

Since q is strictly concave, the condition $\max_{s \in (0, n)} q(s) > 0$ is satisfied if and only if the global maximum is positive, i.e., $q(s_0) > 0$ (noting that if $s_0 \geq n$, $q(s)$ would be decreasing on $(0, n)$ and negative near n , but the condition $q(s_0) > 0$ covers the parameter requirements for feasibility).

Using the first-order condition $ans_0^{-\alpha} = (\sigma^2/\alpha)s_0$, we evaluate the peak value:

$$\begin{aligned} q(s_0) &= \sigma^2 n - \sigma^2 s_0 - n(as_0^{-\alpha} + b) \\ &= \sigma^2 n - \sigma^2 s_0 - \frac{\sigma^2}{\alpha} s_0 - nb \\ &= \sigma^2 n - \sigma^2 s_0 \left(1 + \frac{1}{\alpha}\right) - nb. \end{aligned}$$

The condition $q(s_0) > 0$ is therefore equivalent to

$$\sigma^2 n - nb > \sigma^2 s_0 \left(1 + \frac{1}{\alpha}\right) \iff 1 - \frac{b}{\sigma^2} > \frac{s_0}{n} \left(1 + \frac{1}{\alpha}\right).$$

Substituting $s_0/n = (a\alpha n^{-\alpha}/\sigma^2)^{1/(\alpha+1)}$ yields the final condition:

$$\frac{b}{\sigma^2} < 1 - \left(1 + \frac{1}{\alpha}\right) \left(\frac{a\alpha n^{-\alpha}}{\sigma^2}\right)^{1/(\alpha+1)}.$$

□

Proof of Lemma 1

Proof of Lemma 1. Denote $\psi(\mathbf{X}, Y; \boldsymbol{\theta}) = \nabla_{\boldsymbol{\theta}} l(\mathbf{X}, Y; \boldsymbol{\theta})$. Denote

$$\boldsymbol{\eta}(\boldsymbol{\theta}) = \frac{1}{n-s} \sum_{i=1}^{n-s} \left(\psi(\mathbf{X}_i, Y_i; \boldsymbol{\theta}) - \psi(\mathbf{X}_i, f^{(s)}(\mathbf{X}_i); \boldsymbol{\theta}) \right) + \frac{1}{m} \sum_{j=1}^m \psi(\tilde{\mathbf{X}}_j, f^{(s)}(\tilde{\mathbf{X}}_j); \boldsymbol{\theta}).$$

Then the first order condition of (7) can be written as

$$\boldsymbol{\eta}(\hat{\boldsymbol{\theta}}) = \frac{1}{n-s} \sum_{i=1}^{n-s} \left(\psi(\mathbf{X}_i, Y_i; \hat{\boldsymbol{\theta}}) - \psi(\mathbf{X}_i, f^{(s)}(\mathbf{X}_i); \hat{\boldsymbol{\theta}}) \right) + \frac{1}{m} \sum_{j=1}^m \psi(\tilde{\mathbf{X}}_j, f^{(s)}(\tilde{\mathbf{X}}_j); \hat{\boldsymbol{\theta}}) = 0.$$

We can apply the Taylor's expansion on $\boldsymbol{\eta}(\hat{\boldsymbol{\theta}})$ around the true parameters $\boldsymbol{\eta}(\boldsymbol{\theta}^*)$, such that

$$\hat{\boldsymbol{\theta}} - \boldsymbol{\theta} \approx - \left[\mathbf{J}_{\boldsymbol{\eta}}(\boldsymbol{\theta}^*) \right]^{-1} \boldsymbol{\eta}(\boldsymbol{\theta}^*),$$

where $\mathbf{J}_{\boldsymbol{\eta}}(\boldsymbol{\theta}^*)$ stands for the Jacobian matrix of $\boldsymbol{\eta}(\cdot)$ evaluated at $\boldsymbol{\theta}^*$. Applying the Delta method, we know that the asymptotic variance of $\hat{\boldsymbol{\theta}}$ is

$$\text{Var}(\hat{\boldsymbol{\theta}}) = \mathbb{E} \left[\mathbf{J}_{\boldsymbol{\eta}}(\boldsymbol{\theta}^*) \right]^{-1} \text{Var} \left(\boldsymbol{\eta}(\boldsymbol{\theta}^*) \right) \mathbb{E} \left[\mathbf{J}_{\boldsymbol{\eta}}(\boldsymbol{\theta}^*) \right]^{-1}.$$

Note that,

$$\begin{aligned} \mathbb{E} \left[\mathbf{J}_{\boldsymbol{\eta}}(\boldsymbol{\theta}^*) \right] &= \mathbb{E} \left[\mathbf{H}_{\boldsymbol{\theta}} l(\mathbf{X}, Y; \boldsymbol{\theta}^*) - \mathbf{H}_{\boldsymbol{\theta}} l(\mathbf{X}, f^{(s)}(\mathbf{X}); \boldsymbol{\theta}^*) + \mathbf{H}_{\boldsymbol{\theta}} l(\tilde{\mathbf{X}}, f^{(s)}(\tilde{\mathbf{X}}); \boldsymbol{\theta}^*) \right] \\ &= \mathbb{E} \left[\mathbf{H}_{\boldsymbol{\theta}} l(\mathbf{X}, Y; \boldsymbol{\theta}^*) \right], \end{aligned}$$

where $\mathbf{H}_{\boldsymbol{\theta}} l(\mathbf{X}, Y; \boldsymbol{\theta}^*)$ stands for the Hessian matrix of $l(\mathbf{X}, Y; \boldsymbol{\theta})$ evaluated at $\boldsymbol{\theta}^*$, and the second equality is because \mathbf{X}_i from the small labeled dataset and $\tilde{\mathbf{X}}_j$ from the large unlabeled dataset are sampled from the same distribution.

Note also that,

$$\text{Var} \left(\boldsymbol{\eta}(\boldsymbol{\theta}^*) \right) = \frac{1}{n-s} \text{Var} \left(\psi(\mathbf{X}, Y; \boldsymbol{\theta}^*) - \psi(\mathbf{X}, f^{(s)}(\mathbf{X}); \boldsymbol{\theta}^*) \right) + \frac{1}{m} \text{Var} \left(\psi(\tilde{\mathbf{X}}, f^{(s)}(\tilde{\mathbf{X}}); \boldsymbol{\theta}^*) \right).$$

Because we have a large unlabeled dataset, the second term is approximately zero when m is much larger than $n-s$.

Putting the above together, the asymptotic distribution of $\hat{\boldsymbol{\theta}}$ is

$$\hat{\boldsymbol{\theta}} \sim \mathcal{N}(0, \mathbf{H}^{-1} \mathbf{V} \mathbf{H}^{-1}),$$

where

$$\begin{aligned} \mathbf{H} &= \mathbb{E} \left[\mathbf{H}_{\boldsymbol{\theta}} l(\mathbf{X}, Y; \boldsymbol{\theta}^*) \right], \\ \mathbf{V} &= \frac{1}{n-s} \text{Var} \left(\psi(\mathbf{X}, Y; \boldsymbol{\theta}^*) - \psi(\mathbf{X}, f^{(s)}(\mathbf{X}); \boldsymbol{\theta}^*) \right) + \frac{1}{m} \text{Var} \left(\psi(\tilde{\mathbf{X}}, f^{(s)}(\tilde{\mathbf{X}}); \boldsymbol{\theta}^*) \right) \end{aligned}$$

□

EC.2. A Ramp-up Procedure to Fit Scaling Law

So far we have discussed the optimal sample allocation when the constants in the scaling law are known. In this section, we propose a data-driven ramp-up procedure to estimate the parameters in the scaling law.

We start with an overview of our procedure. We randomly partition the n samples of the small labeled dataset into three disjoint subsets: an FT subset, a validation subset, and a PPI subset. First, we use samples from the FT subset to fine-tune the LLM predictor $f^{(s)}(\cdot)$. Second, we use samples from the validation subset to estimate the parameters in the scaling law. Third, we use samples from the PPI subset, together with the fine-tuned predictor $f^{(s)}(\cdot)$, to estimate $\hat{\mu}$.

Now we introduce some notation to rigorously define this procedure. Let the ramp-up procedure proceed in $k \geq 3$ stages. Let the sample size of the validation subset be n_v , which does not depend on k . We randomly draw n_v samples from the labeled dataset \mathcal{N} to form the validation subset \mathcal{N}_v . We keep this validation sample \mathcal{N}_v unchanged during the ramp-up procedure.

Recall that the ramp-up procedure proceeds in k stages. Let there be a k -grid of sample sizes $\{n_1, n_2, \dots, n_k\}$ such that $0 < n_1 < \dots < n_k < n - n_v$. From the remaining labeled data $\mathcal{N} \setminus \mathcal{N}_v$, we randomly draw a nested sequence of samples

$$\emptyset \subset \mathcal{N}_1 \subset \mathcal{N}_2 \subset \dots \subset \mathcal{N}_k \subset \mathcal{N} \setminus \mathcal{N}_v,$$

with $|\mathcal{N}_\ell| = n_\ell$. (One way to generate this nesting is to first draw \mathcal{N}_k from $\mathcal{N} \setminus \mathcal{N}_v$ and then subsample to obtain $\mathcal{N}_{k-1}, \dots, \mathcal{N}_1$.)

In stage $\ell \in [k]$, we fine-tune a predictor $f^{(n_\ell)}(\cdot)$ on sample \mathcal{N}_ℓ . After obtaining the predictor $f^{(n_\ell)}(\cdot)$, we evaluate the residual variance $\text{Var}(Y - f^{(n_\ell)}(\mathbf{X}))$ using the fixed validation set \mathcal{N}_v . Denote the validation residuals by

$$r_i^{(\ell)} := Y_i - f^{(n_\ell)}(\mathbf{X}_i), \quad (\mathbf{X}_i, Y_i) \in \mathcal{N}_v.$$

We estimate the mean residual and residual variance on \mathcal{N}_v by

$$\begin{aligned} \hat{\theta}_{(1),\ell} &:= \bar{r}^{(\ell)} = \frac{1}{n_v} \sum_{(\mathbf{X}_i, Y_i) \in \mathcal{N}_v} r_i^{(\ell)}, \\ \hat{\theta}_{(2),\ell} &:= \widehat{\text{Var}}_{\mathcal{N}_v}(r^{(\ell)}) = \frac{1}{n_v - 1} \sum_{(\mathbf{X}_i, Y_i) \in \mathcal{N}_v} (r_i^{(\ell)} - \hat{\theta}_{(1),\ell})^2. \end{aligned}$$

After obtaining the sample variance estimator, we collect a pair of $(n_\ell, \hat{\theta}_{(2),\ell})$.

We will then use all the pairs collected up to stage ℓ , namely $\{(n_\iota, \hat{\theta}_{(2),\iota})\}_{\iota=1}^\ell$, to fit a scaling law,

$$(\hat{\alpha}, \hat{a}, \hat{b}) = \arg \min_{\alpha, a, b} \sum_{\iota=1}^{\ell} \left(\hat{\theta}_{(2),\iota} - a n_\iota^{-\alpha} - b \right)^2.$$

Finally, we can plug in the estimated parameters $(\hat{\alpha}, \hat{a}, \hat{b})$ to numerically solve equation (4).

Suppose the solution to equation (4) is calculated as \hat{s}_ℓ^* , and we will use \hat{s}_ℓ^* to guide the ramp-up decision. If both $\ell < k$ and $\hat{s}_\ell^* > n_\ell$, we proceed with the ramp-up procedure, and go to stage $\ell + 1$. If either $\ell = k$ or $\hat{s}_\ell^* \leq n_\ell$, we stop by setting $s = n_\ell$. We then use all the remaining samples $\mathcal{N} \setminus (\mathcal{N}_v \cup \mathcal{N}_\ell)$ as the small labeled dataset to perform PPI and obtain the estimator $\hat{\mu}$.

Note that, the validation subset is neither used to fine-tune the LLM predictor $f^{(s)}(\cdot)$, nor used by the PPI to estimate $\hat{\mu}$. To save samples, we could remove the validation subset and use cross-validation in each \mathcal{N}_l , for $l \in [k]$, to evaluate $\text{Var}(Y - f^{(n_l)}(\mathbf{X}))$.

EC.3. Additional Empirical Analysis

EC.3.1. Scaling Law Robustness Check

To ensure that our scaling law-guided allocation is reliable in practice, we assess the robustness of the estimated parameters against two primary sources of uncertainty: data sampling and training randomness.

Let ω denote a generic quantity derived from the scaling law fit, such as the parameter vector (a, α, b) or the resulting optimal allocation ratio s^*/n . We decompose the total variability of ω using the Law of Total Variance:

$$\text{Var}(\omega) = \underbrace{\text{Var}_D(\mathbb{E}_\epsilon[\omega | D])}_{\text{Data Sampling}} + \underbrace{\mathbb{E}_D(\text{Var}_\epsilon(\omega | D))}_{\text{Training Randomness}}, \quad (\text{Eq.4})$$

where D represents the specific labeled dataset split and ϵ captures stochasticity arising from model initialization and optimization. The first term quantifies sensitivity to the specific sampling of the fine-tuning data, while the second term captures variability induced by stochastic optimization when the dataset is held fixed.

Bootstrap Procedure. We approximate this decomposition using a two-level resampling design. Specifically, from the held-out pool we first draw $B_D = 10$ independent datasets $\{D_1, \dots, D_{10}\}$ of size 5,000. For each D_j , we rerun the fine-tuning and scaling-law fitting under $B_\epsilon = 5$ different random seeds, yielding $\omega_{j,k}$ for $k = 1, \dots, 5$ and a total of $B_D \times B_\epsilon = 50$ fitted outcomes. To form the reported robustness intervals, we then apply a nonparametric bootstrap over these 50 fitted outcomes: we resample with replacement 1,200 times and recompute the corresponding summary statistic (median fit/parameters and the implied s^*/n) in each bootstrap draw. The 95% robustness interval is given by the 2.5th and 97.5th percentiles of the resulting bootstrap distribution.

Robustness of the scaling law fit. Figure EC.1 visualizes the robustness of the fitted scaling law under bootstrap resampling. Each light curve corresponds to one bootstrap replicate, while the solid line represents the median scaling law fit across replicates. The shaded region indicates the central 95% robustness interval. Despite noticeable dispersion in the individual parameter estimates

(a, α, b) , the fitted curves remain tightly clustered across the full range of fine-tuning subset sizes. This demonstrates a high degree of robustness—the scaling law captures a fundamental relationship between data size and variance reduction.

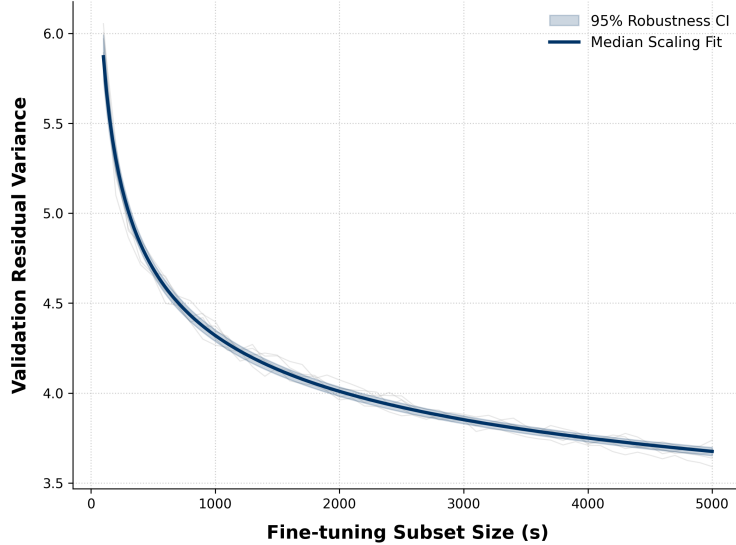


Figure EC.1 Bootstrap robustness of the scaling law fit estimated with $n = 5,000$ labeled samples. Light curves correspond to individual bootstrap replicates, the solid line denotes the median fit, and the shaded region indicates the central 95% robustness interval.

Parameter-level robustness and implied allocation. The results are further quantified in Table EC.1, which summarizes the bootstrap robustness of the estimated parameters and the implied optimal allocation ratio across 2,000 replicates. While individual parameters (a, α, b) show small to moderate dispersion with R^2 around 0.996, the optimal allocation ratio s^*/n , remains remarkably stable with a narrow 95% robustness interval.

Table EC.1 Bootstrap robustness of scaling law parameters and implied optimal allocation, estimated with $n = 5,000$ labeled samples

Quantity	Median	95% Confidence Interval
Scaling parameter a	11.403	[9.678, 13.937]
Scaling parameter α	0.261	[0.203, 0.318]
Variance floor b	2.447	[1.938, 2.761]
Optimal allocation s^*/n	0.110	[0.105, 0.114]
Fit quality (R^2)	0.996	[0.993, 0.998]

These findings provide strong empirical evidence that the scaling law provides a robust foundation for allocation decisions. The stability of s^*/n confirms that the resulting allocation rule is resilient to both data sampling and training randomness, supporting its reliability in practical estimation and inference tasks.

EC.3.2. Few-shot Prompt for PPI-Only Estimator

For the PPI-ONLY estimator, we cannot use the raw LLM embeddings directly, e.g., Qwen3-Embedding-0.6B with the MLP regression head. Instead, we employ a few-shot prompt strategy (illustrated in Figure EC.2) where the valid score range (80–100) and demonstration examples are provided in the context window to guide the base LLM’s (GPT-5-nano) generation.

```
--- SYSTEM PROMPT---
I will provide a wine review.
Rate the described wine at scale of 80--100 based on the wine review.

Here are two examples of how to rate:

Review:
This is a walk backward after the impressive 2012. Almost impenetrably black, the flavors converge
around espresso and bitter chocolate, yet the tannins have a green edge. The wine simply feels
flat in the mouth with no life to it.
Rating: 85

Review:
This is one of the great Rieslings from the Wachau, a wonderful panoply of ripe, tropical fruit,
pierced with flint, spice and minerality. It is rich and opulent, while never losing sight of
the core tautness of a fine Riesling.
Rating: 95

--- USER PROMPT---
Now, please rate the following review:

Herbal aromas, a chunky palate and herbal cherry and plum flavors finish earthy and with a raisiny
element. This is sort of amorphous and mealy on the palate.

--- LLM OUTPUT ---
Rating: 83
```

Figure EC.2 Few-shot prompt used to obtain LLM surrogates for the PPI-Only estimator in the Wine Reviews study.

EC.3.3. Comparison of Fine-Tuning Objectives

We analyze the behavior of the fine-tuned LLM on the validation set to explain the performance differences observed in the main analysis. As established in Proposition 2, the efficiency of the PPI estimator is primarily governed by the coefficient of determination $R^2(s)$, or equivalently, the magnitude of the residual variance $\text{Var}(Y - f^{(s)}(\mathbf{X}))$. Therefore, achieving a lower residual variance is a necessary condition for improved downstream inference.

Figure EC.3 compares the validation residual variance of LLMs fine-tuned with our proposed variance loss (\mathcal{L}_{var}) versus those trained with the standard MSE loss across varying subset sizes s . For reference, we include a baseline representing the variance of a constant predictor (the mean of training ratings). The results demonstrate that the variance-based objective consistently achieves

lower residual variance than MSE. This advantage is particularly pronounced in the small- s regime. While MSE attempts to minimize total error (conflating bias and variance), our objective explicitly targets the conditional spread of prediction errors. By decoupling variance reduction from MSE minimization, the model specializes in the specific metric that drives PPI efficiency, leaving the bias correction to the subsequent rectification step.

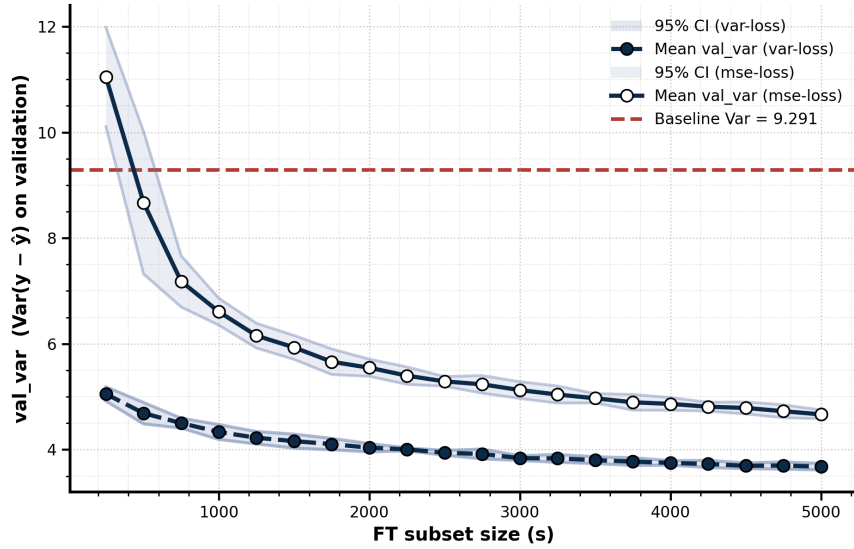


Figure EC.3 Validation residual variance under variance-based and MSE-based fine-tuning.

EC.4. Extension: Independent but Non-Identical Fine-Tuning Data

In the main paper, we have focused on a single labeled dataset \mathcal{N} and a single unlabeled dataset \mathcal{M} drawn from the target distribution, and studied how to optimally allocate the n target labels between fine-tuning and PPI.

In many real applications, however, practitioners also have access to additional labeled data that are *independent* but not necessarily *identically distributed* with the target task. For example, in a survey study, it is common to have a large archive of previous questionnaires and responses across products, features, and customer segments, and then to field a new survey on a specific question of interest. One can first fine-tune an LLM on the archive of prior surveys and responses, and then use that fine-tuned LLM as a starting point for a new product study with limited labels on the new questionnaire; see, e.g., Brand et al. (2023). This is an “independent but non-identical” setting: the prior surveys are not drawn from the same distribution as the new question, but they provide useful prior information about how to map text responses to numerical outcomes.

In the following, we show that our framework naturally accommodates such extra fine-tuning data, and that the optimal sample allocation on the new task remains valid under mild independence assumptions.

Setup with external fine-tuning data. We extend the main setup as follows. In addition to the target-task labeled and unlabeled datasets

$$\mathcal{N} = \{(X_i, Y_i)\}_{i=1}^n, \quad \mathcal{M} = \{\tilde{X}_j\}_{j=1}^m,$$

drawn i.i.d. from $(X, Y) \sim \mathcal{F}$ and $X \sim \mathcal{F}_X$ as before, we assume there is an extra labeled dataset

$$\mathcal{H} = \{(X_k^{\text{ext}}, Y_k^{\text{ext}})\}_{k=1}^{N_{\text{ext}}},$$

with an *arbitrary* joint distribution (not necessarily equal to \mathcal{F}), such that

$$\mathcal{H} \perp\!\!\!\perp (\mathcal{N}, \mathcal{M}).$$

The data in \mathcal{H} may come from previous survey questions, different products, or other related tasks.

A training algorithm \mathcal{A} takes as input the external dataset \mathcal{H} and s labeled examples from the new task, say $\mathcal{N}_{\text{FT}} \subset \mathcal{N}$ with $|\mathcal{N}_{\text{FT}}| = s$, and outputs a fine-tuned predictor

$$f^{(s)} = \mathcal{A}(\mathcal{H}, \mathcal{N}_{\text{FT}}) : \mathcal{X} \rightarrow \mathcal{Y}.$$

The remaining $n - s$ target labels

$$\mathcal{N}_{\text{PPI}} = \mathcal{N} \setminus \mathcal{N}_{\text{FT}}$$

are reserved for PPI. The PPI estimator on the new task is then

$$\hat{\mu}^{(s)} = \frac{1}{n-s} \sum_{(X_i, Y_i) \in \mathcal{N}_{\text{PPI}}} (Y_i - f^{(s)}(X_i)) + \frac{1}{m} \sum_{j=1}^m f^{(s)}(\tilde{X}_j). \quad (\text{Eq.5})$$

The key structural assumption is that the data used to build $f^{(s)}$, namely $(\mathcal{H}, \mathcal{N}_{\text{FT}})$, are independent of the data used for PPI, namely $(\mathcal{N}_{\text{PPI}}, \mathcal{M})$; their marginal distributions can differ.

PROPOSITION EC.1 (Unbiasedness and variance with external fine-tuning data).

Assume:

- (a) (X_i, Y_i) are i.i.d. from $(X, Y) \sim \mathcal{F}$ for $i = 1, \dots, n$; \tilde{X}_j are i.i.d. from $X \sim \mathcal{F}_X$ for $j = 1, \dots, m$, independent of $\{(X_i, Y_i)\}_{i=1}^n$;
- (b) \mathcal{H} is an arbitrary labeled dataset, independent of $(\mathcal{N}, \mathcal{M})$;
- (c) for a given s , the predictor $f^{(s)}$ is a measurable function of $(\mathcal{H}, \mathcal{N}_{\text{FT}})$ only, with \mathcal{N}_{FT} and \mathcal{N}_{PPI} forming a partition of \mathcal{N} of sizes s and $n - s$.

Then the estimator $\hat{\mu}^{(s)}$ defined in (Eq.5) satisfies

$$\begin{aligned} \mathbb{E}[\hat{\mu}^{(s)}] &= \mathbb{E}[Y], \\ \text{Var}(\hat{\mu}^{(s)}) &= \frac{1}{n-s} \text{Var}(Y - f^{(s)}(X)) + \frac{1}{m} \text{Var}(f^{(s)}(X)), \end{aligned}$$

where the expectations and variances are taken with respect to the target distribution \mathcal{F} of (X, Y) .

Proof of Proposition EC.1. We condition on the fine-tuning data $(\mathcal{H}, \mathcal{N}_{\text{FT}})$, which fixes the predictor $f^{(s)}$. By assumption (a) and the independence assumption (b), the datasets \mathcal{N}_{PPI} and \mathcal{M} remain independent of $f^{(s)}$ and consist of i.i.d. draws from \mathcal{F} and \mathcal{F}_X , respectively.

First, we establish unbiasedness. Using the linearity of expectation and the fact that $f^{(s)}$ is fixed conditionally:

$$\begin{aligned} \mathbb{E}[\hat{\mu}^{(s)} | f^{(s)}] &= \frac{1}{n-s} \sum_{(X_i, Y_i) \in \mathcal{N}_{\text{PPI}}} \mathbb{E}[Y_i - f^{(s)}(X_i) | f^{(s)}] + \frac{1}{m} \sum_{j=1}^m \mathbb{E}[f^{(s)}(\tilde{X}_j) | f^{(s)}] \\ &= \mathbb{E}[Y - f^{(s)}(X) | f^{(s)}] + \mathbb{E}[f^{(s)}(X) | f^{(s)}] \\ &= \mathbb{E}[Y] - \mathbb{E}[f^{(s)}(X)] + \mathbb{E}[f^{(s)}(X)] \\ &= \mathbb{E}[Y]. \end{aligned}$$

By the Law of Iterated Expectations, $\mathbb{E}[\hat{\mu}^{(s)}] = \mathbb{E}[\mathbb{E}[\hat{\mu}^{(s)} | f^{(s)}]] = \mathbb{E}[\mathbb{E}[Y]] = \mathbb{E}[Y]$.

Next, we derive the variance. Applying the Law of Total Variance:

$$\text{Var}(\hat{\mu}^{(s)}) = \mathbb{E}[\text{Var}(\hat{\mu}^{(s)} | f^{(s)})] + \text{Var}(\mathbb{E}[\hat{\mu}^{(s)} | f^{(s)}]).$$

From the unbiasedness result above, the conditional expectation $\mathbb{E}[\hat{\mu}^{(s)} | f^{(s)}] = \mathbb{E}[Y]$ is a constant (the true population mean). Therefore, the second term $\text{Var}(\mathbb{E}[\hat{\mu}^{(s)} | f^{(s)}]) = 0$.

We now compute the first term. Conditional on $f^{(s)}$, the summands in (Eq.5) are independent. Thus, the conditional variance is:

$$\begin{aligned} \text{Var}(\hat{\mu}^{(s)} | f^{(s)}) &= \text{Var}\left(\frac{1}{n-s} \sum_i (Y_i - f^{(s)}(X_i)) \middle| f^{(s)}\right) + \text{Var}\left(\frac{1}{m} \sum_j f^{(s)}(\tilde{X}_j) \middle| f^{(s)}\right) \\ &= \frac{1}{n-s} \text{Var}(Y - f^{(s)}(X) | f^{(s)}) + \frac{1}{m} \text{Var}(f^{(s)}(X) | f^{(s)}). \end{aligned}$$

Taking the expectation over $f^{(s)}$ (which is equivalent to the definition of the variance terms in the problem setup), we obtain the final result. \square

Proposition EC.1 shows that our variance decomposition in (2) holds without change when the fine-tuning procedure uses additional independent data from other tasks. All that matters for the PPI variance on the new task is how well the resulting $f^{(s)}$ predicts $(X, Y) \sim \mathcal{F}$.

Scaling law and optimal allocation with external data. In the main development, we assume that for the *target* task there exist constants $a > 0$, $\alpha > 0$, and $b \geq 0$ such that the residual variance of $f^{(s)}$ obeys the scaling law

$$\text{Var}(Y - f^{(s)}(X)) \approx as^{-\alpha} + b,$$

when $f^{(s)}$ is obtained by fine-tuning on s independent target labels. In the extended setting above, the same assumption is interpreted *conditional on* the external data \mathcal{H} : for a given external fine-tuning procedure and resulting starting model, there exist a, α, b such that the residual variance

on the new task decays as s increases, and the quality of the external data is reflected in these parameters. For example, using a rich archive of prior surveys will typically reduce b and increase α .

Under this interpretation, the variance approximation in the large- m regime remains

$$\text{Var}(\hat{\mu}^{(s)}) \approx \frac{as^{-\alpha} + b}{n - s},$$

and the optimal sample allocation problem on the *new* task is unchanged: we still choose $s \in (0, n)$ to minimize $(as^{-\alpha} + b)/(n - s)$. This is exactly the same expression in (4). All previous results, including Theorem 1 and Propositions 1–3 hold here.

In other words, our method continues to require labeled data from the new task for both fine-tuning (to move along the scaling curve) and for PPI (to debias the predictions). Additional independent labeled data from other tasks can be freely used to improve the starting point of the model; their effect is summarized by a more favorable scaling law on the new task. As long as the scaling law is estimated using labeled data from the new task (via the ramp-up procedure in Online Appendix EC.2), the same allocation rule remains statistically optimal for that task, regardless of how much extra independent fine-tuning data were available upstream.